12-2021

Assessing the Effectiveness and Efficacy of Wireless Onboard Condition Monitoring Modules in Identifying Defects in Railroad Rolling Stock

Lee R. Cantu
The University of Texas Rio Grande Valley

ASSESSING THE EFFECTIVENESS AND EFFICACY OF WIRELESS ONBOARD

CONDITION MONITORING MODULES IN IDENTIFYING

DEFECTS IN RAILROAD ROLLING STOCK

A Thesis

by

LEE R. CANTU

Submitted in Partial Fulfillment of the

Requirements for the Degree of

MASTER OF SCIENCE IN ENGINEERING

Major Subject: Mechanical Engineering

The University of Texas Rio Grande Valley

December 2021

ASSESSING THE EFFECTIVENESS AND EFFICACY OF WIRELESS ONBOARD

CONDITION MONITORING MODULES IN IDENTIFYING

DEFECTS IN RAILROAD ROLLING STOCK

A Thesis
by
LEE R. CANTU

COMMITTEE MEMBERS

Dr. Constantine Tarawneh
Chair of Committee

Dr. Heinrich Foltz
Committee Member

Dr. Arturo Fuentes
Committee Member

Dr. Stephen Crown
Committee Member

December 2021

ABSTRACT

Cantu, Lee R., <u>Assessing the Effectiveness and Efficacy of Wireless Onboard Condition Monitoring Modules in Identifying Defects in Railroad Rolling Stock.</u> Master of Science in Engineering (MSE), December, 2021, 84 pp., 9 tables, 47 figures, references 33 titles.

Many industries have begun shifting into the Internet of Things (IoT) in the 21st century. To help ease this transition for the rail industry, The University Transportation Center for Railway Safety (UTCRS) has partnered with Hum Industrial Technology, Inc. (HUM) to help complete the development of a Wireless Onboard Condition Monitoring system named the 'Boomerang™'. This product allows customers to schedule proactive maintenance on their railcars to replace defective wheels and/or bearings, saving them time, money and potentially preventing costly catastrophic derailments. The UTCRS research team has established thresholds to determine defective bearings utilizing thermal and mechanical sensors.

The effectiveness and efficacy of the Boomerang™ devices to identify different types of defects on bearings were tested and compared against validated UTCRS wired and wireless sensor modules. Laboratory testing was performed on dynamic bearing test rigs that mimic rail service operation. Additionally, a methodical temperature calibration was performed for the Boomerang™ to predict bearing operating temperatures to within 8°C for a wide range of operating conditions. After a few optimization cycles followed by a functionality verification, 40 Boomerangs were assembled and deployed for a field pilot test. Results of the pilot test confirm the Boomerang™ readiness for field service implementation.

DEDICATION

The completion of this thesis is dedicated to my family. Mom and Dad, I would not be where I am today without the unconditional love and support from both of you. To my mother, Flor, thank you for making sure your sons and daughter always had everything we needed to be successful and for teaching us long life skills. To my father, Edelmiro, thank you for always providing for our family. Dad, thank you for teaching me how to be a hard worker and to earn my success. Mom and Dad, thank you for constantly pushing me to be better and for being such great role models. To my brother and sister, thank you for always looking up so highly to me and for constantly pushing each other to be better. El esfuerzo de este trabajo es por ustedes ama y apa, los amo.

ACKNOWLEDGMENTS

TABLE OF CONTENTS

LIST OF TABLES

LIST OF FIGURES

CHAPTER I

BACKGROUND AND INTRODUCTION

With the railroad industry's rise to prominence in North America during the 1800s [1], there has been enduring improvement in its development as a dependable and reliable industry. However, with many derailments occurring year after year in North America, organizations like the United States Department of Transportation (USDOT) and its Federal Railroad Administration (FRA) as well as the Association of American Railroads (AAR) have established numerous regulations to safeguard against these disastrous and costly events [2][3]. From 2011 to 2020, there have been 1673 derailments on American railroads related to mechanical or electrical failures as reported by the FRA [4]. The FRA reported that 8.3% of those derailments were related to journal bearing failure, resulting in billions of dollars in fees and damages for private investors. To put this in perspective, the estimated cost of rail incidents in North Carolina totaled about $2.4 billion USD from the years 2010 to 2019 [5]. A derailment could cost a private railroad investor $25,000 to $250,000 an hour to restore any resulting damage based on the severity of the incident [6]. As reported by the AAR, there is an average annual investment of $25 billion to help maintain infrastructure, equipment, and technology to provide a safer railroad environment [7].

Being the highest percentage cause of mechanical failure derailments in North America, tapered-roller bearings, shown in Figure 1 [8], have been closely studied and evaluated to understand the phenomena leading to their catastrophic failure.

Typical tapered-roller bearings consist of three main components: the outer ring (cup), inner ring (cone), and the rollers, as depicted in Figure 1. Commonly, after operating hundreds of thousands of miles, or in rare cases, shortly after being set into operation, bearings have been known to develop defects or overheating issues that can render them inoperable and can ultimately lead to train derailments.
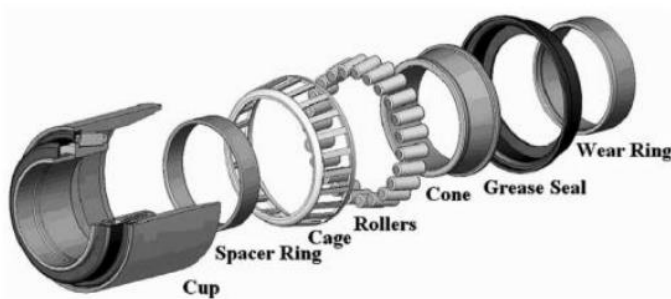
Figure 1: Tapered-roller bearing exploded view [8]

Tapered-roller bearing defect types can be categorized as distributed defects, localized defects, or geometric defects. Spalls, cracks, and pits are examples of localized defects. Distributed defects can be found on multiple components such as the cup, cone, or rollers with localized defects, or a single component with numerous defects distributed throughout its surface, such as a water-etch defect pictured in Figure 2.

Figure 2: Tapered-roller bearing defects

Geometrical defects usually result from irregularities or faults in the manufacturing process which can cause one or more of the bearing components to be out of tolerance. Depending on the severity of the geometric defects, they can lead to abnormal bearing operation and enhanced frictional heating which manifests in higher bearing operating temperatures, and in extreme cases, may cause the bearing to fail catastrophically resulting in a bearing burn-off.

Upon reviewing the common causes behind the premature cessation of a bearings' service life, it is now relevant to discuss the preventative measures that allow freight operators to safely replace them. Wayside monitoring systems and track equipment have been among the foremost railroad technologies utilized, and have reduced the number of derailments by mechanical failures and train accidents by 33% since the start of the 21st century [7]. As previously mentioned, journal bearing failures are the most common cause of mechanical failure

derailments, which brought about the implementation of common wayside technologies such as Acoustic Bearing Detectors (ABD) and Hot Box Detectors (HBD) back in the 1960s.

Trackside Acoustic Bearing Detector Systems (TADS™) function by analyzing the acoustic frequencies produced by the different components of a bearing including the cup, cone, and rollers [9]. Utilizing wayside microphones, TADS™ can detect high-risk defects in bearings and alert the train operator. "Growlers" and "water-etch pitting" are the most common high-risk defects detected by TADS™. These are defects that occupy about 90% of the bearing rolling surfaces. With only nineteen operational TADS™ in North America, they must be positioned appropriately. TADS™ are designed to operate in areas where the railcar travels more than 40 mph without applying brakes. TADS™ can detect end-of-life bearings with high proficiency but cannot detect bearings with minor defect sizes. Moreover, TADS™ cannot detect inner ring (cone) defects with the same accuracy and reliability as outer ring (cup) defects. RailBAM® is a different type of ABD that functions like the TADS™. The main difference is that RailBAM® can also detect wheel impacts using tie-mounted auxiliary sensors and a trackside receiver. Contrary to the TADS™, the RailBAM® can detect defective bearings on a railcar and track the propagation of a defect using radiofrequency. However, with only 20 operational RailBAM® and a total of 39 ABDs in North America, most bearings will run their entire service life without passing through any of these systems [10].

These acoustic detection systems have their own limitations and fall short in detecting overheating issues in bearings that generate little if any acoustic feedback. With over 6000 units of Hot Box Detectors (HBDs) in North America, HBDs can distinguish overheating journal bearings using infrared thermal technology [11]. Tapered-roller bearings operating with cup (outer ring) temperatures greater than 94.4°C (170°F) above ambient conditions or 58.3°C

(105°F) hotter than their mate bearing on the same wheel-axle are flagged and scheduled for replacement and removal to be inspected. Overheating journal bearings can result in a bearing burn-off and cause a derailment within 1 to 3 minutes. Since most HBD are placed anywhere between 40 and 64 rail kilometers (25-40 rail miles) apart, a bearing burn-off can occur between HBDs without much advance notice. Moreover, bearing operating temperature is a function of load and speed, i.e., while some bearings might overheat at high load and speed, they might run normally at empty railcar loads and slower speeds. Researchers have also determined that some defective bearings can run undetected by HBDs because the bearing operating temperature is underestimated by these devices [12]. Finally, it is important to note that not every defective bearing overheats [13].

Bearings flagged by HBDs are removed from service and sent to specialized facilities to be inspected. Upon teardown and inspection, bearings that show no evidence of any of the common causes of bearing failure are classified as "non-verified". A study conducted by one of the major railroad bearing manufacturers in North America concluded that about 40% of bearings flagged by HBDs between 2001 and 2007 were non-verified bearings. Reducing the number of false positives flagged by HBDs is paramount in mitigating the associated costly and unnecessary train stoppages and delays resulting in rail operation downtime.

While wayside technologies have been instrumental in decreasing the number of derailments caused by journal bearings, these technologies are hindered by limitations such as the intermittent and/or inconsistent monitoring of assets coupled with the reactive nature of these systems. The shortcomings of the currently deployed wayside technologies in rail service has sparked the research efforts into innovative continuous onboard condition monitoring systems for rail rolling stock.

Over the past decade, researchers at the University Transportation Center for Railway Safety (UTCRS) have been working on developing and optimizing an onboard condition monitoring system for railroad tapered-roller bearings. Normal operation performance thresholds for bearing temperature and vibration signatures have been established based on the operating load and speed of the bearing [14]. The onboard condition monitoring system circuitry incorporates an accelerometer and a temperature sensor that are mounted onto the bearing's steel adapter. The preliminary prototype was a wired system that has been extensively tested and validated in the laboratory and proven to accurately and reliably detect bearing defects at their early stage of initiation. The functionality of this wired system has also been verified in the field through limited testing carried out at the Transportation Technology Center, Inc. in Pueblo, Co [15].

Since a wired version of this onboard condition monitoring system would not be feasible for implementation in freight rail service, a wireless onboard condition monitoring module was developed and tested against the wired prototype to ensure that the wireless module is as efficient in detecting faults in rolling stock. The development of the UTCRS wireless onboard condition monitoring module was aided by recent technological advances in micro-processing units, lithium-ion batteries, and wireless communications.

The onboard condition monitoring prototypes developed by the UTCRS research team caught the attention of Hum Industrial Technology, Inc. (HUM), a private rail industry, who licensed the technology and developed their own prototype wireless onboard condition monitoring system called the "Boomerang" because of its shape. HUM contracted the UTCRS research team to assist in further development and optimization of the "Boomerang". This work entailed extensive laboratory testing and validation coupled with the development of a

temperature sensor calibration correlation that accurately predicts the bearing operating temperature from sensor readings taken at the bearing adapter. The work also included iterative design improvements based on the laboratory test findings. Finally, the HUM prototype Boomerang™ was deployed in a carefully planned pilot field test to assess its efficacy in monitoring the health of railroad rolling stock and identifying defective components.

This thesis presents the work performed to optimize the HUM Boomerang™ and assess its efficacy in accurately and reliably determining the condition of railroad bearings in rail service operation. Chapter II provides a thorough literature review of the earlier works to develop onboard condition monitoring systems along with a summary of their advantages and disadvantages. In Chapter III, a detailed description will be given of the experimental setup and instrumentation used to perform the laboratory testing as well as the Boomerang™ deployment setup utilized for the pilot field test. Chapter IV describes the experimental work performed resulting in the iterative design enhancement process of the Boomerang™ and the calibration correlation development for the Boomerang™ temperature sensor In Chapter V, the results of the pilot field test carried out on a Class II rail track are discussed along with the findings of the experimental testing conducted on the bearings removed from service. Finally, Chapter VI summarizes the conclusions of this study and discusses the readiness of the HUM Boomerang™ wireless onboard condition monitoring system for field service deployment.

CHAPTER II

LITERATURE REVIEW

Over the past 50 years, the number of derailments caused by mechanical failures has

decreased largely due to the ongoing research conducted by the rail industry, however, the

collateral damage resulting from derailments is still a clear and present issue. Although Hot-Box

Detectors (HBDs) were implemented in the 1960s as a means to identify overheating bearings,

they remain unreliable and still yield non-verified bearings (i.e., false positives), which

ultimately results in increased operational costs due to labor expenses and associated train

stoppages and delays. On the contrary, Trackside Acoustic Detector Systems (TADS™) are

more accurate in identifying bearings that are near the end of their service life but are inept in

detecting defects that are in early stages of development or small defects located in the inner ring

raceways of bearings. As expressed in Chapter 1, the next evolution in asset health monitoring is

to apply wayside detection system technologies towards smart onboard condition monitoring

systems that can continuously report rolling stock performance metrics and assess their health.

However, the idea of onboard systems is not novel as efforts to develop onboard monitoring

systems began in the mid-1970s. A summary of some of the relevant earlier works in this area is

presented hereafter. In 1976, Armstrong [16] patented a bearing temperature actuated sensor to

automatically apply the railcar brake system when a bearing begins to exceed normal operating

temperature. The temperature sensor, shown in Figure 3, is secured to the bearing adapter at the

position labeled "10". When it detects abnormal temperatures, it sends a signal to preemptively activate the brake line and automatically stop the railcar prior to causing further damage.
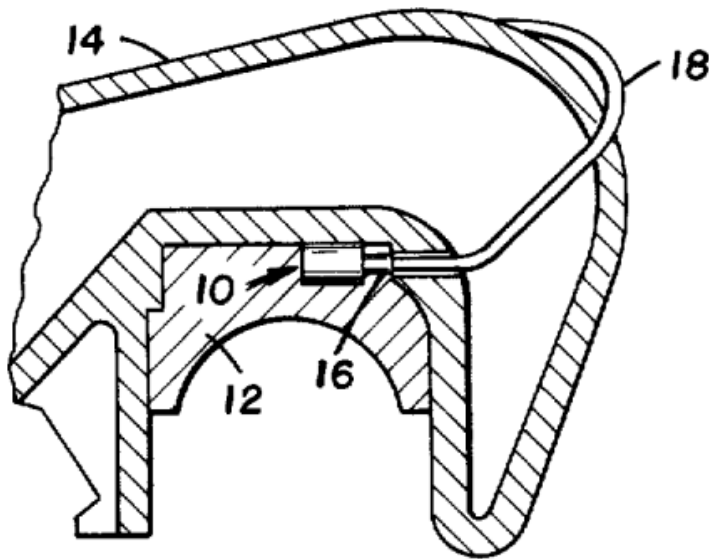
Figure 3: Journal bearing derailment prevention system temperature sensor location [16]

While Armstrong's system was able to identify overheated bearings, it had a serious drawback. When an overheated bearing was detected, the system would overrule the authority of the railcar operator, stopping the railcar without their consent. Moreover, the automatic nature of the braking system is plagued by issues related to false positive detections. In some cases, bearings may exhibit a sharp rise in temperature as they begin their operation but slowly cool down to normal levels as steady-state operating conditions prevail. Sudden increases in operating temperature are not always indicative of a defective bearing. Hence, Armstrong's system was susceptible to false positives which rendered it financially impractical when considering the unnecessary maintenance stops and delays on the rail tracks.

In 1987, R. Newman [17] developed the SmartBolt™ device which was designed as a warning system, completely contained in a single bolt, that would alert crew members on the train about an overheated bearing. Every bearing is secured in place by an end cap, which is fastened by three screw bolts, as pictured in Figure 4.
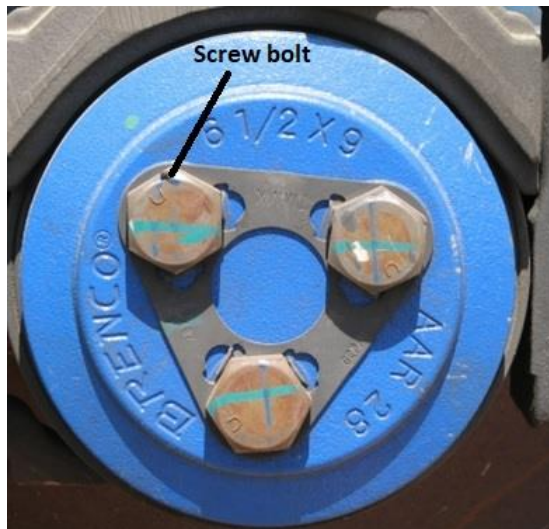
Figure 4: End cap screw bolt locations [18]

Advances in technology allowed for the SmartBolt™ to be integrated with complex mechanisms, as shown in Figure 5. These mechanisms include an actuator, a thermal sensor, a power source, and a transmitter. The SmartBolt™ actuator is activated by an expanding wax motor when established temperature thresholds are surpassed. The temperature thresholds are based on the journal bearings weakest temperature resistant component. After expanding the actuator, an antenna emerges from the bolt head as a visual indicator for the overheated bearing, and simultaneously transmits a signal. The receiver alerts the train crew about a faulty bearing which is then scheduled for maintenance. The SmartBolt™ must then be replaced, as the structure of the bolt is compromised when engaging the antenna.
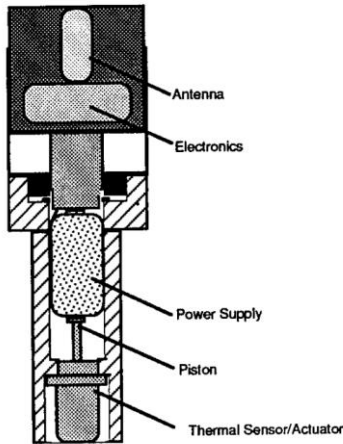
Figure 5: SmartBolt™ electronic housing cross section [17]

After developing a working prototype, the SmartBolt™ was tested in a laboratory and

verified in a field test at the Transportation Technology Center, Inc. (TTCI) in Pueblo, Colorado.

Tested under normal operating conditions, the SmartBolt™ contained two different wax motors

that actuated at temperatures of 13°C (55°F) and 27°C (80°F). Shortly after beginning the initial

field test, the first SmartBolt™ activated at 48 km/h (30 mph), and the second activated after

traveling at a speed of 64 km/h (40 mph) for 21 minutes. The next steps in finalizing the

SmartBolt™ were to optimize the mechanical properties of the bolt containing the electronics,

and to mass-produce the device at a competitive price. Even though the product performed to

expectations, there were some lingering challenges to overcome. The SmartBolt™ is activated

by brief temperature spikes which, as explained earlier, are not always indicative of a faulty

bearing. Nevertheless, once activated, the SmartBolt™ antenna will deploy and a signal will be

transmitted even if the temperature reverts to safe or normal values. Unfortunately, when the

train operator receives the transmitted signal, that triggers a scheduled train stoppage to replace

the compromised SmartBolt™ regardless of whether the associated bearing is healthy or faulty.

Despite its shortcomings, the SmartBolt™ set a standard for onboard temperature monitoring devices and inspired innovation in this field.

The introduction of the Wireless Sensor Nodes (WSNs) in the 21st century evolved onboard condition monitoring systems. WSNs comprise an always-online onboard monitoring system that communicates wirelessly to a transmitter (a gateway or a central monitoring unit) to convey the bearing condition to a server [19]. WSNs will then allow for the bearing condition to be continuously monitored and evaluated by the railcar owner so that maintenance on their railcars can be scheduled at their own discretion in the interest of preventing damages caused by derailments.

In 2003, Timken Co. developed a self-powered onboard monitoring system by integrating technology in a different form-factor. The Timken Guardian™ was a monitoring solution that doubled as an internal component for tapered-roller bearings [20]. The Guardian™ communicates with an external receiver by means of radio signals to continuously monitor bearing health. The primary advantage of the Guardian™ is the fast response time associated with directly measuring the temperature of the bearing. Figure 6 shows how the Guardian™ replaces the inner spacer ring of a tapered-roller bearing, which was introduced in Chapter I, Figure 1.
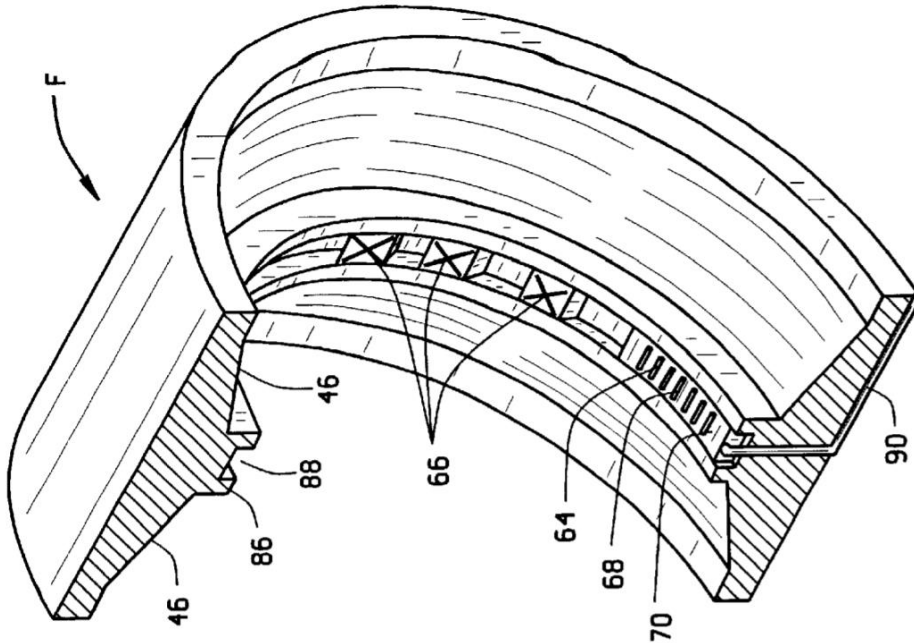
Figure 6: Timken Guardian™ Bearing [20]

The Guardian™ is composed of several components including a transmitter, onboard processor, thermal and vibration sensors, and a power supply. A primary concern for the Timken Guardian™ is that electrical components tend to fail under higher temperatures. Commercial electric elements are rated with a maximum operating temperature of 120°C (248°F). Accelerometer performance is inversely proportional to operating temperature, resulting in lower fidelity at higher temperatures, because they are calibrated under ambient conditions [21]. The Timken Guardian™ was never field tested and never progressed past the prototypical phase of development. Like the SmartBolt™, the Guardian™ is not a reusable device and is essentially married to the bearing in which it is embedded. The success of the device would have been dependent on its cost and availability when replacing an axle assembly. This prompted the development of an onboard monitoring system whose function is not interrupted when a wheel-axle assembly is replaced.

13

IONX, a subsidiary of Amsted Rail, developed a temperature-based bearing condition monitoring system. The system, named IONX EDGE™, was verified and tested extensively by members of the UTCRS research team before being subjected to a field validation test in March 2010 in Australia [22]. Zagouris [23] devised an IONX EDGE™ WSN specific temperature correlation for the bearing operating temperature, which accounts for the indirect placement of the temperature sensor on the bearing adapter. Figure 7 shows the layout of the IONX EDGE™ WSN and its placement on the bearing steel adapter.

Figure 7: IONX EDGE™ WSN module [20]

Zagouris concluded that by implementing his correlation, the predicted bearing operating temperature was within ±10°C (±18°F) of the actual bearing temperature. The derived temperature correlation was based on a wide variety of defective and control (healthy) bearings. Numerous sets of laboratory experiments utilizing AAR class K, F, E, and G bearings were conducted at different speed and load operating conditions. Two main loading conditions were used simulating a fully loaded and an empty railcar with testing speeds ranging from 40 km/h (25 mph) to 137 km/h (85 mph).

In the Australia field test, the IONX EDGE™ modules were used to assess the health of tapered-roller bearings based on predetermined temperature thresholds. Each module was independently powered by two high-performance lithium-ion batteries and was secured to the bearing adapters via four fine thread bolts, as seen in Figure 7. A total of 124 class E bearings were continuously monitored for six months, and their temperature data was collected and analyzed. IONX actively monitored these bearings using a dedicated server that received the data via satellite through a Communication Management Unit (CMU) mounted on each test railcar [24]. Two bearings had abnormal temperature behavior which resulted in their removal from service. These bearings were then sent to the UTCRS for further laboratory testing and subsequent teardown and inspection which validated their removal from service.

IONX merged with Amsted Rail to create Amsted Digital Solutions (ADS). ADS claims that they have added more than just temperature monitoring on railcars by utilizing enhanced present-day technology that was not previously available [25]. Without disclosing their technology, ADS states that they have developed predictive analytics tools to assess the health of wheel and bearing components.

Although operating temperature is one of the indicators of bearing health, it is a reactive metric, i.e., by the time the operating temperature has increased significantly indicating a fault, the bearing is at the end of its service life, thus necessitating immediate action resulting in costly train stoppages and delays to avoid catastrophic derailments. Bearing vibration signatures are a better indicator of bearing health because they can signal the onset of a bearing defect and can be used to efficiently track the defect deterioration, thus offering early alarms allowing railcar owners to schedule proactive maintenance when convenient.

Motivated by the aforementioned, the UTCRS research team sought to develop a vibration-based condition monitoring device that can detect the onset of bearing failure. The first iteration of this device is a wired system that acquires the vibration signatures of bearings in operation via an accelerometer and records the data utilizing a National Instruments (NI) data acquisition system for further analysis [15]. Additionally, an algorithm was developed that uses the Root Mean Square (RMS) values of the collected vibration signatures to distinguish between healthy and defective bearings. Appropriate RMS threshold values were determined through extensive laboratory testing performed using a large library of healthy and defective bearings of class F, K, E, and G [15][26]. These RMS thresholds have been refined and validated through exhaustive laboratory testing and have been found to be speed dependent [15][26]. The developed algorithm was optimized using the refined RMS thresholds and additional features were added to allow the algorithm to identify defective bearings, the defect type (i.e., cup, cone, or roller defect), and the approximate size of the defect [15][26]. After establishing proof of concept using the wired onboard accelerometers shown in Figure 8, the UTCRS research team completed a field test at TTCI in 2015 [27].
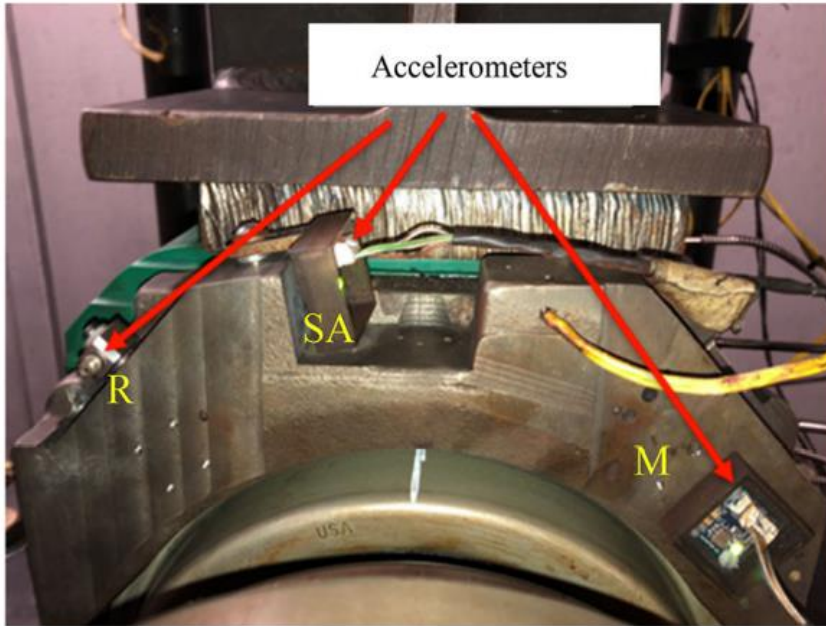
Figure 8: UTCRS wired onboard condition monitoring system [27]

In the 2015 TTCI field test, a total of eight bearings were tested. Half of the bearings were defective, and the other half were control (defect-free) bearings. In this blind test, the wired accelerometers in conjunction with the devised health assessment algorithm were able to detect and identify the four defective bearings at different speed and load combinations in the field environment. Moreover, the algorithm could also determine the defect type and its approximate size [15].

Even though the wired onboard monitoring system was validated in field operation during the 2015 TTCI pilot test, it is not feasible to incorporate a wired system across a train of freight railcars. This study proved that the algorithm developed by the UTCRS research team can effectively and reliably assess the bearing health and can detect defective bearings operating in rail service. However, these findings also highlighted the need for a self-powered wireless onboard system.

Motivated by this, the UTCRS research team embarked on designing a wireless version of their initial wired system that was extensively validated in the laboratory and in the field. The wireless solution developed by the UTCRS research team offers both vibration and temperature monitoring and utilizes low-power electronics that process the acquired data and transmit it to a central monitoring unit via Bluetooth connectivity. A picture of the wireless onboard sensor module is shown in Figure 9.

Figure 9: UTCRS wireless onboard condition monitoring module and power source [28].

The wireless onboard condition monitoring system requires more power when sending dense data packets. This can quickly drain the battery power supply when sampling data at longer sample intervals. Cuanang [28] optimized the defect-detection algorithm to function using one-second sample data to minimize power consumption while maintaining the same level of efficacy and reliability as the wired system.

Although several companies claim to have developed systems that assesses the bearing and wheel health of freight train railcars, the majority of these companies refuse to disclose the technology behind their solutions. Most of the emergent monitoring solutions, such as the system

developed by ADS, feature over six years of maintenance-free operation, the ability to function in harsh environments, low-power consumption, and active GPS tracking for freight trains [25]. Other than bearing and wheel health monitoring, some of these companies claim that their devices can also provide railcar load status, braking state, temperature levels, and hatch position. However, no real data or quantifiable evidence have been offered to substantiate their claims.

Other companies like RailPulse™ have incorporated a data gathering system promoting the advancement of Positive Train Control (PTC) systems [29]. PTC is designed to reduce the number of derailments caused by unauthorized railcar movement, excessive speed, and incorrect track switches [30]. However, PTC does not prevent any derailments or incidents caused by equipment failure, train operator errors, and other human error based causes. RailPulse™ is on the verge of creating a cloud-based system that includes PTC and other technology that can determine equipment failure.

Lat-Lon® developed a solar-powered system that measures the impact or shift in g-force as felt by the railcar, along with bearing temperature, humidity, and pressure. The system can also report these values directly with its locomotive monitoring unit [31]. With many more companies on the verge of accomplishing this feat, such as ZTR Control Systems, Wi-Tronix LLC, Progress Rail, Ondas Network, and nVent, only a few can provide proven bearing and wheel health condition monitoring solutions. Journal bearing health condition is not the focus of every emergent onboard monitoring system, however, as mentioned in Chapter I, journal bearings are the leading cause of mechanical equipment failure derailments.

Armed with that knowledge, the UTCRS partnered with Hum Industrial Technology, Inc. (HUM) to develop their predictive wheel and bearing condition monitoring system. As a result, HUM created a low-power, durable, wireless onboard system with live GPS fleet-

tracking, leak detection, and automated safety monitoring that can predict wheel and bearing failures months in advance [32]. The evaluation of the HUM system in both laboratory and field conditions is discussed throughout the following chapters of this thesis, where the experimental setup and testing apparatus will be described in detail. The ensuing results prove the efficacy and reliability of this wireless onboard condition monitoring solution in determining the health of railcar wheels and bearings in rail service as validated by a pilot field test.

CHAPTER III

LABORATORY AND FIELD TEST EXPERIMENTAL SETUP

3.1 Laboratory Test Rigs

The University Transportation Center for Railway Safety (UTCRS) dynamic bearing test rigs housed at the University of Texas Rio Grande Valley were used to conduct the experimental testing for this study. The objectives of the experimental testing were three-fold, namely: (1) develop an accurate and reliable transfer function that correlates the Boomerang sensor temperature taken on the bearing adapter to the actual bearing operating temperature, (2) assess the performance of the Boomerang and its ability to accurately identify defective bearings under different combinations of load and speed operating conditions, and (3) make recommendations for design improvements and performance enhancements based on the extensive laboratory testing performed on the Boomerang prototype devices.

The dynamic bearing test rigs are designed to mimic the operating conditions experienced by railroad tapered-roller bearings in rail service. The laboratory experiments were carried out utilizing two types of testers, the single bearing tester (SBT) and the four-bearing chamber tester (4BCT). Both types of testers can run four distinct classes of railroad bearings, namely: Class E (6"×11 "), Class F (6$\frac{1}{2}$"×12 "), Class G (7"×12 "), and Class K (6$\frac{1}{2}$"×9 "). Each bearing class has its dimensions and rated load capacity listed in Table 1 in accordance with the Association of American Railroads (AAR) standards.

Table 1: AAR standards for bearing dimensions and load capacities per bearing class

Bearing Class	Size [mm]	Size [in]	Load [kN]	Load [kips]
Class E	152×278	6"×11 "	117	26.3
Class F	165×305	$6\frac{1}{2}$"×12 "	153	34.4
Class G	178×308	7"×12 "	169	38.0
Class K	165×229	$6\frac{1}{2}$"×9 "	153	34.4

Each dynamic bearing test rig is equipped with a hydraulic cylinder capable of applying up to 150% of the rated operating load of any bearing class. An Arduino-based load controller automatically adjusts the active load to be within ±1% of the desired load by collecting 52 samples of the active load every second and activating the hydraulic transducer to correct any deviation. The terms 17% load and 100% load, as referenced throughout this thesis, refer to a standard load applied to the bearing. For example, the class K and F bearings are rated for a load of 153 kN (34.4 kips), which represents a 100% fully loaded railcar, whereas a load of 26 kN (5.85 kips) per bearing corresponds to an empty railcar load or equivalently 17% of the full railcar load.

The SBT and 4BCT use a 22 kW (30 hp) variable frequency motor to rotate bearings at equivalent speeds up to 137 km/h (85 mph). The variable frequency driver (VFD) allows the motor to operate at wide variety of revolutions per minute (rpm), which correspond to the speeds listed in Table 2. The test rigs are equipped with two industrial-size fans that can produce an average air velocity of 6 m/s (13.4 mph) to supply forced convection on the bearings. One of the main differences between the SBT and the 4BCT is that the 4BCT is housed in a temperature-

controlled environmental chamber that allows for the ambient to be maintained at any temperature in the range from -40 to 65°C (-40 to 150°F). In contrast, the SBT operates in room temperature ambient conditions. Moreover, unlike the 4BCT, the SBT can apply lateral and impact loads to the test bearing. Common laboratory practice is to utilize the SBT for short-duration testing since the test bearing can be readily replaced with minimal effort, while the 4BCT is mainly used for long-duration experiments such as service life performance testing.

Table 2: Variable frequency motor RPM to track speed conversion table

Axle Speed [rpm]	Track Speed [km/h]	Track Speed [mph]
234	40	25
280	48	30
327	56	35
374	64	40
420	72	45
467	80	50
498	85	53
514	89	55
560	97	60
618	106	66
700	121	75
796	137	85

3.1.1 Single Bearing Tester (SBT)

The SBT, pictured in Figure 10, has a cantilever arrangement that closely emulates the way a railcar bearing sits at the end of the wheel-axle. This tester can accommodate one class E, F, G, or K tapered-roller bearing at a time.
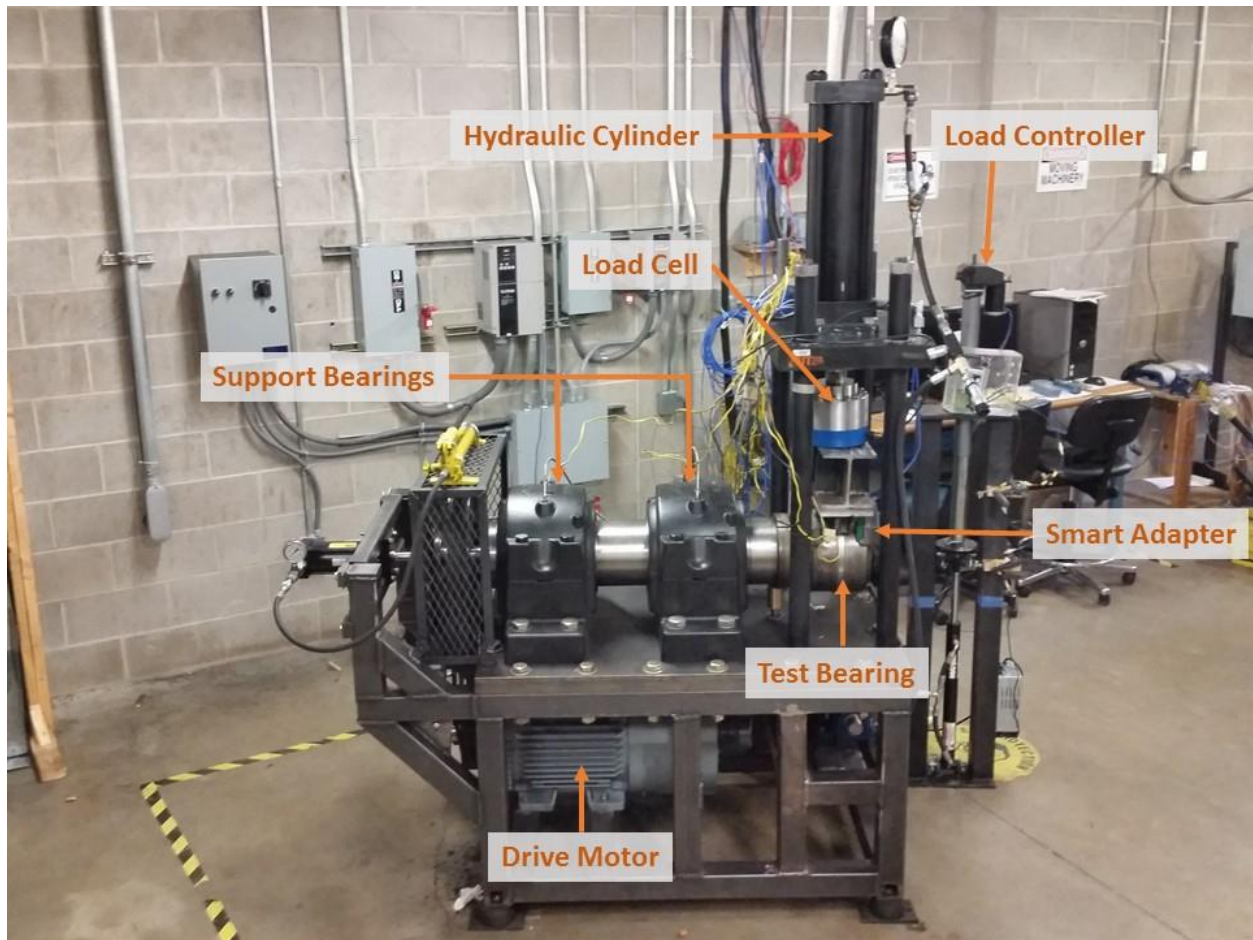
Figure 10: UTCRS Single bearing tester (SBT)

The hydraulic cylinder provides a vertical load ensuring that the bearing is top-loaded, which exactly matches field conditions. The SBT can simulate train traveling speeds of up to 106 km/h (66 mph) and can also provide higher speeds of up to 137 km/h (85 mph) but for short durations. One of the main advantages of the SBT is that it can replicate wheel flats and bad

track segments utilizing a specially designed impact mechanism. The impact mechanism can simulate an 83.8 cm (33") wheel defect at 29 km/h (18 mph) or a 91.4 cm (36") wheel defect at 32 km/h (20 mph) using a 3 Hz frequency (i.e., 3 impacts per second).
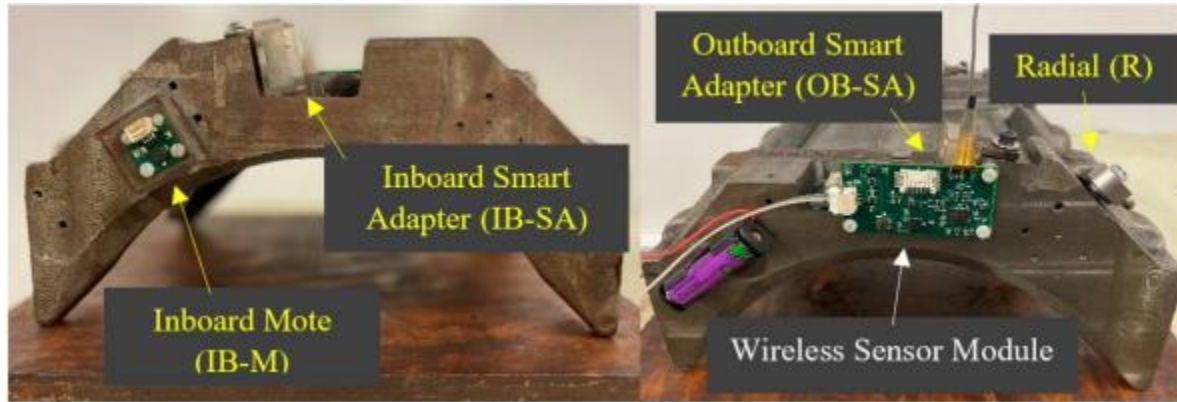
Figure 11: Sensor positions on smart adapter

Figure 11 details the positions of the different accelerometers affixed to the bearing adapter. The term "smart" is used to imply the sensor technologies implemented on the bearing adapter. Three wired single-axis 100g analog accelerometers (ADXL) are optimally placed to collect vibration signatures within the bearing. The outboard smart adapter (OB-SA) accelerometer is centered with respect to the adapter to accurately measure the vertical vibrations of the bearing at the top center location. Similarly, the inboard side of the adapter is also instrumented with an inboard smart adapter ADXL (IB-SA). Moreover, the inboard mote location (IB-M) accelerometer measures the radial vibration signatures within the bearing as the cone and rollers transition from the top loaded region of the bearing to the unloaded zone. At the outboard side of the adapter, a wired PCB 500g accelerometer is mounted on the slanted part of the adapter and oriented so that it measures the radial vibration signatures of emitting from the bearing. This accelerometer is used as a secondary reference to the IB-M wired accelerometer. Finally, the single-axis 100g analog accelerometer used in the UTCRS wireless module is like

those used in the three wired devices. The bearing adapter has been machined so that the wireless module can be mounted either in the SA or the M locations to allow for a direct comparison of its performance relative to the wired accelerometer devices. Note that the terms inboard and outboard refer to the two sides of the bearing adapter that face the wheel side and the end-cap side, respectively.

3.1.2 Four-Bearing Chamber Tester (4BCT)

As mentioned earlier, the 4BCT, shown in Figure 12, is normally used for long duration testing such as that required for service life performance testing of bearings. Simulated train traveling speeds of up to 137 km/h (85mph) can be maintained throughout the long duration testing with no need for maintenance. It is common practice to perform a complete teardown and visual inspection on the test axle and the four test bearings every 96,560 km (60,000 miles) of continuous operation to ensure that no defects have developed on any of the components and to check the condition of the lubricating grease. Following this inspection, if no issues are found, the test axle setup with the four bearings are re-assembled using the same components and grease as before the teardown.
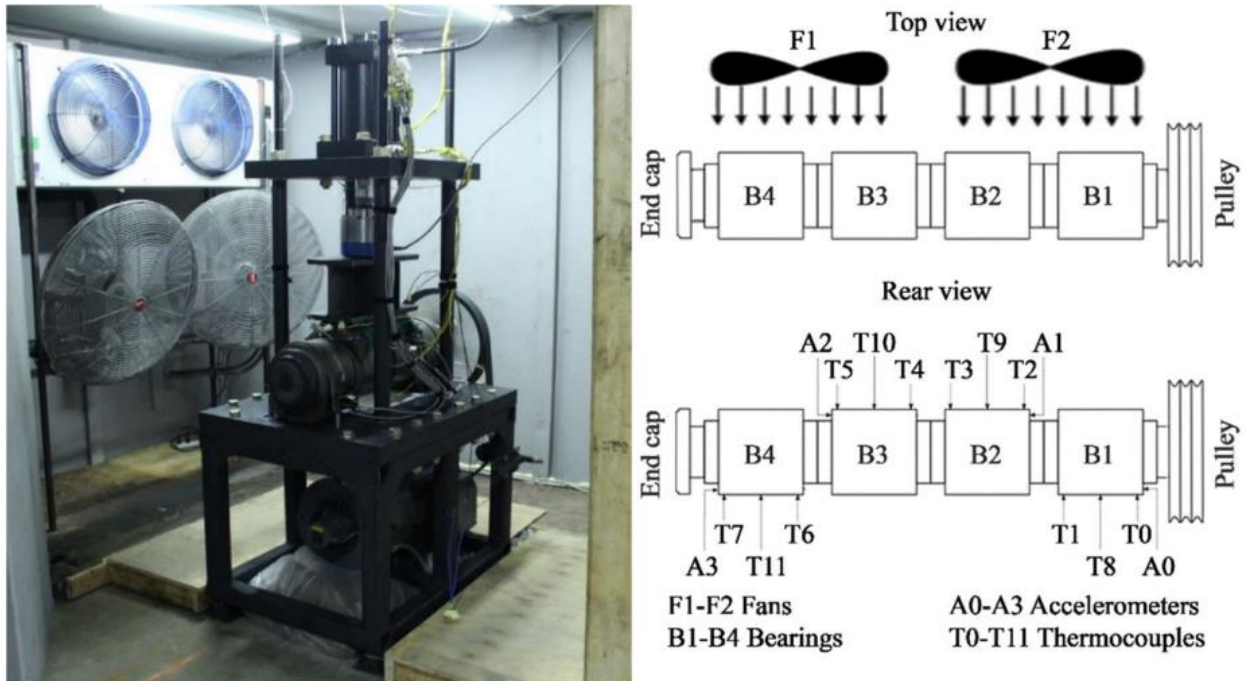
Figure 12 : Four-bearing chamber tester and bearing arrangement schematic diagram

From the schematic diagram of Figure 12, bearing positions B2 and B3 are top-loaded just like in rail service, while bearings B1 and B4 are bottom-loaded and thus serve as control bearings. The two top-loaded bearing adapters are specially machined to accommodate two 100 g accelerometers in the smart adapter (SA) and mote (M) locations, and a 500 g PCB accelerometer in the radial (R) position, as depicted in Figure 13. Figure 14 shows the locations of two spring-loaded bayonet-style K-type thermocouples, along with the single K-type thermocouple that is clamped firmly against the outside surface of the bearing cup (outer ring) midway along its length via a hose clamp. The average value of the three temperature readings acquired from these K-type thermocouples provides the bearing operating temperature.
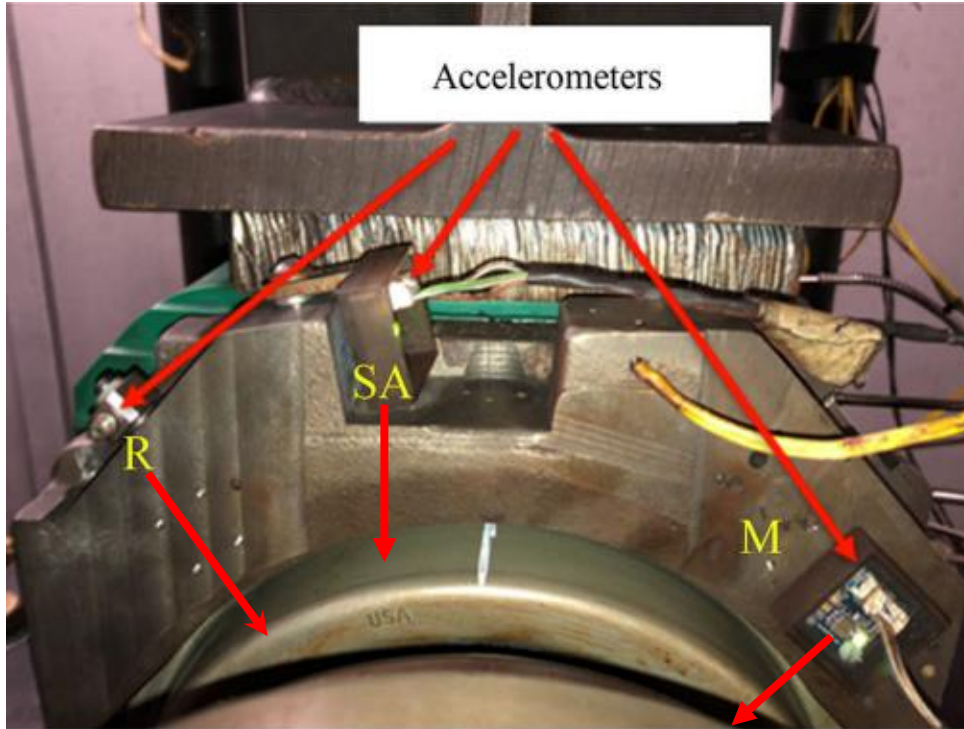
Figure 13 : 4BCT smart adapter accelerometer sensor locations and measuring directions
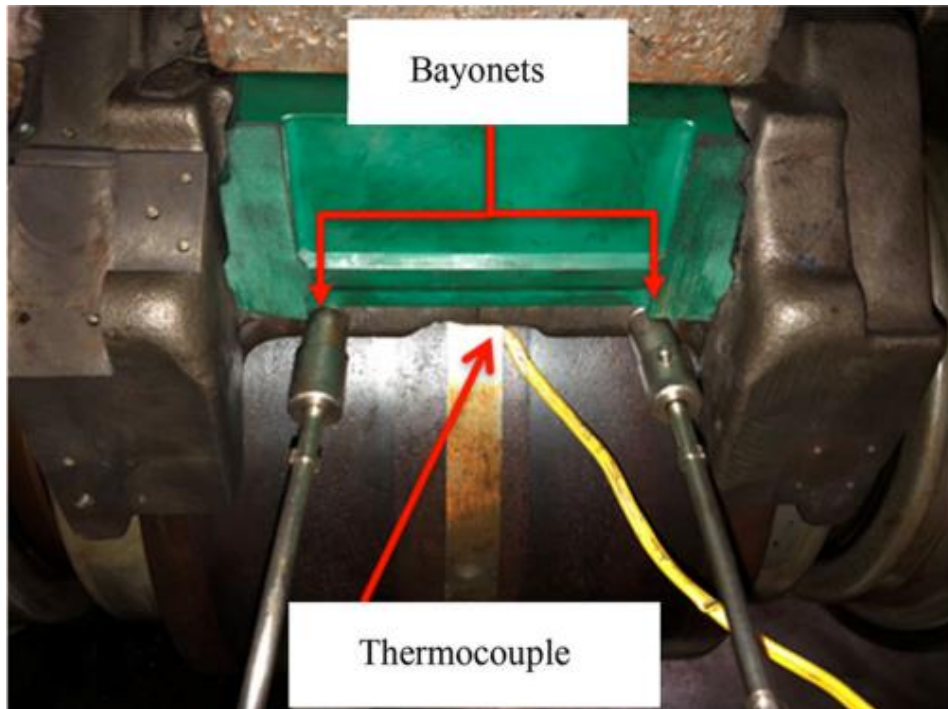
Figure 14: 4BCT bayonet and thermocouple locations

3.1.3 Data Acquisition System

The data acquisition systems (DAQ) used for the SBT and 4BCT are National

Instruments (NI) DAQs programmed utilizing the engineering software LabVIEW™. The SBT

uses a NI PXIe-1062Q DAQ while the 4BCT uses a NIcDAQ-9174 DAQ. As the data are

processed and collected by their respective DAQ systems, LabVIEW™ then records data files

with the accelerometer and thermocouple measurements which can be accessed for data analysis

using the mathematical software MATLAB™.

Using a NI TB-2627 card for the SBT and a NI-9213 card for the 4BCT, temperature data

measured using the thermocouples was sampled at 128 Hz for half-second periods every twenty

second intervals. The LabVIEW™ user interface (UI) monitors live temperature data to observe

the thermal behavior of the bearing in real time.

The wired accelerometer data is collected at a sampling rate of 5,120 Hz for sixteen

seconds every ten minutes for both the SBT and the 4BCT. The SBT utilizes an 8-channel NI

PXI-4472B card, whereas the 4BCT uses a combination of NI-9239, NI-9235, and NI USB-6008

cards to acquire the accelerometer data. LabVIEW™ was programmed to instantaneously plot

the vibration signatures acquired by the accelerometers and calculate and display the root-mean-

square (RMS) values of the raw vibration signals in g's (gravitational acceleration) using a

conversion based on the calibrated sensitivity of the specific accelerometer. Similarly, the

recorded data files from LabVIEW™ are then extracted and the analysis is performed utilizing

the mathematical software MATLAB™ to generate vibration and temperature profile plots.

The UTCRS wireless module uses a Raspberry PI 3 Model B+ to collect the

accelerometer data in ten-minute intervals at a sampling rate of 5,200 Hz for one or four second

periods via Bluetooth. The acquired data is downloaded from the Raspberry PI and MATLAB™

is used to calculate the RMS values which are compared against the reference wired accelerometer data.

3.2 HUM Technology Onboard Condition Monitoring Module Setup

The Boomerang™ functions together with the "Gateway" to perform as a wireless sensor node (WSN). Figure 15 shows the central communication unit named the Gateway. The Gateway houses several communication sensors and, more importantly, can transmit data to a Hum Industrial Technology Inc. (HUM) server via a cellular modem. The Gateway device requires no maintenance and is sustainable through solar power. The Boomerang shown in Figure 16 is designed to meet the geometrical limitations of Class K and Class F bearing adapters. Inside the Boomerang, a single axis 100g accelerometer is centrally aligned with the bearing adapter. This centerline is indicated by the red arrow, which matches the orientation of the UTCRS wired accelerometer in the SA location.

Figure 15: HUM central communication unit (i.e., Gateway)
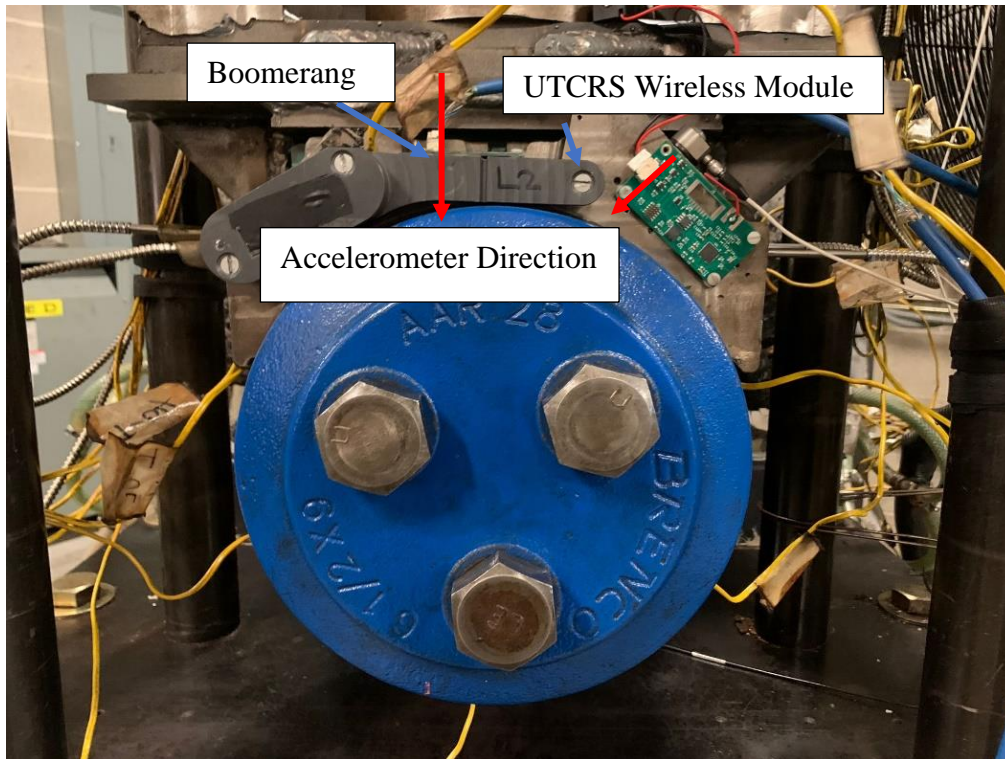
Figure 16: Smart Adapter equipped with a HUM Boomerang and a UTCRS wireless module

3.2.1 Boomerang Revisions

The HUM Boomerang underwent several design iterations, and each subsequent design was validated through laboratory testing. Three versions of the Boomerang were tested on the SBT and 4BCT using several healthy and defective bearings with varying defect severity. The Boomerang prototype development began with computer aided designs (CADs) created on SOLIDWORKS™ and plastic prototypes were 3D-printed to verify fitness on Class K and Class F adapters. As demonstrated in Figure 17 and Figure 18, the Boomerang enclosure is incompatible with the older generation of Class K steel adapters but can accommodate both the old and new designs of Class F adapters and the new design of Class K adapters. For laboratory testing purposes, the Boomerang recorded a one-second dataset every 10 minutes at a sampling

rate of 5,200 Hz. However, only the RMS values of the acquired datasets as computed by the

Boomerang firmware were transmitted to the Gateway to minimize battery power consumption.

Figure 17: Fit test on Class K steel adapters; left (new design) and right (old design)
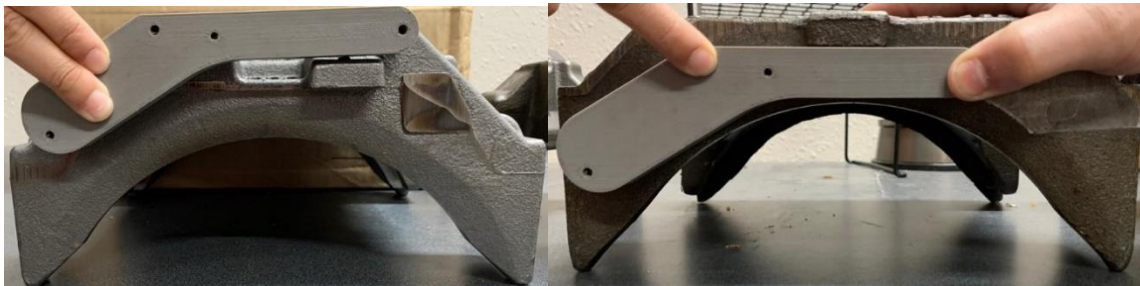
Figure 18: Fit test on Class F steel adapters; left (new design) and right (old design)

3.2.1.A Boomerang A

The first iteration of the Boomerang, Revision A (Rev. A), was evaluated through

laboratory testing by comparing its performance to the UTCRS wired and wireless sensor

modules. The enclosure used for Boomerang A, shown in Figure 19, was mounted directly to the

adapter surface. The Boomerang functionality was verified by running a defective bearing on the

SBT under loaded and unloaded railcar conditions at a velocity of 97 km/h (60 mph). The

defective bearing had a cone spall with a defect area of approximately 11.16 cm^2 (1.73 in^2), as

seen in Figure 20.

Figure 19: Boomerang A enclosure, front view (A), back view (B)

Spall Area = 11.16 cm² (1.73 in²)

Figure 20: Cone spall– Experiment 228B

3.2.1.B Boomerang B

Revision B (Rev. B) improved upon the design of Rev. A with the inclusion of a temperature sensor. The adapter surface temperature is measured using a copper stud that is adhered to the temperature sensor located on the Boomerang circuit board. Boomerang B underwent extensive laboratory testing at various load, speed, and ambient operating conditions to develop the temperature transfer function and to assess its ability to identify defective bearings with varying levels of defect severity.

The Boomerang temperature transfer function was developed by systematically comparing the average bearing operating temperature and the adapter surface temperature measured by the Boomerang temperature sensor via the contacting copper stud. The location of the Boomerang temperature sensor is indicated in Figure 21 with Figure 22 showing the copper stud that makes direct contact with the surface of the bearing adapter. The Boomerang temperature sensor was set to acquire data at the same 128 Hz sampling rate as the K-type thermocouples in Figure 14 where half a second of data was collected every 20 seconds. Note that the data used to devise the transfer function were steady-state temperatures.
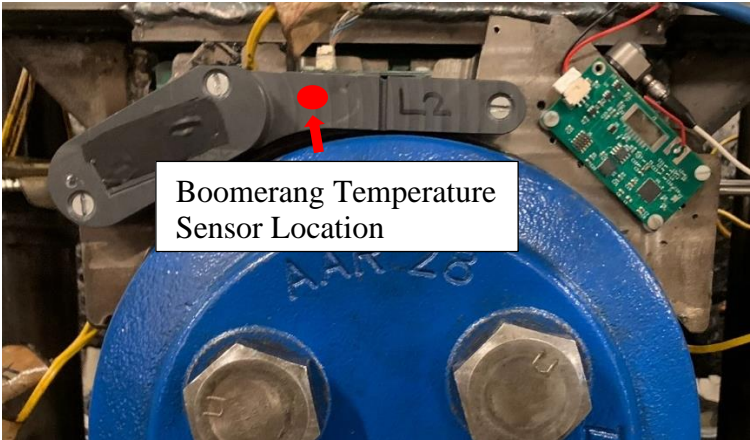
Figure 21: Boomerang temperature sensor location (front side)
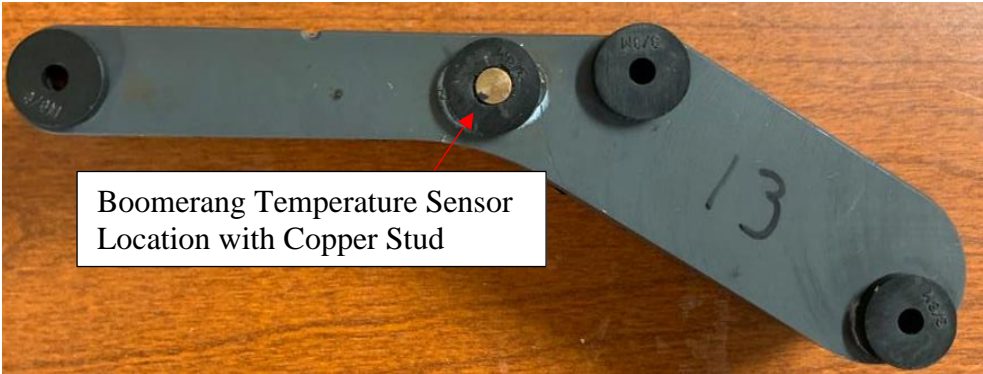
Figure 22: Boomerang temperature sensor location with copper stud (back side)

More than 50 datasets of steady-state bearing operating temperatures and corresponding Boomerang temperature readings were used to develop the polynomial fit (i.e., transfer function)

that predicts the bearing operating temperature (T_p) from the acquired Boomerang temperature. To ensure that this temperature correlation was representative of rail service operating conditions, the 4BCT was used to simulate empty and full railcar loads, with speeds that increased from 40 km/h (25 mph) to 137 km/h (85 mph) in increments of 8 km/h (5 mph). Moreover, the temperature-controlled environmental chamber allowed for a wide range of bearing operating temperatures as low as -8°C (18°F) and as high as 100°C (212°F) by maintaining different chamber ambient temperatures.

3.2.1.C Boomerang C

The third revision of the Boomerang, Revision C, was a restructuring of the onboard condition monitoring module used for complete validation of the accelerometer and temperature sensor performance. In addition to the single-axis 100g accelerometer, Boomerang C implemented a 200g three-axis accelerometer with the purpose of detecting low frequency, high impact loads caused by wheel and track detects. Note that the temperature transfer function that correlates the Boomerang temperature measured at the adapter surface to the bearing operating temperature was undergoing continuous improvement throughout the development cycle and verification testing of the Boomerang.

3.2.2 Field Test Setup and Removal Process

After a few optimizations, 40 Boomerangs were assembled and deployed for a pilot field test. Pictured in Figure 23, a single Gateway was installed per railcar while ensuring proper positioning for optimal solar exposure and clear cellular communications. As mentioned earlier, the Gateway is a solar-powered device that acts as a data relay bridge between the onboard condition monitoring module and the reporting server used by the railcar owner. Specifically, the Gateway receives the data collected by the Boomerang via a LORA transmitter. Then, the rolling

stock health information is transferred into HUM's internet-based server. Here, the data is

analyzed by the server's software which generates an automated email notification when a

temperature or vibration threshold is surpassed, thus indicating a possibly defective bearing or

wheel.

Figure 23 : Gateway field installation on a freight railcar

Before installing the Boomerang as seen in Figure 24, the bearing adapter on the railcar is

modified using basic drill and tap techniques to secure the Boomerang at three specific mounting

locations with threaded screws. Using the latest revision of the Boomerang (Rev. C), the

vibration RMS Level 1 analysis was performed and the bearing operating temperature data was

collected for nine privately owned railcars.

Figure 24 : Boomerang B field installation

Following the Association of American Railroads (AAR) wheel identification diagram, depicted in Figure 25, the Boomerangs were then registered onto HUM's server using their respective installation positions to facilitate the identification of the bearings, wheels, and axles when analyzing the incoming data.
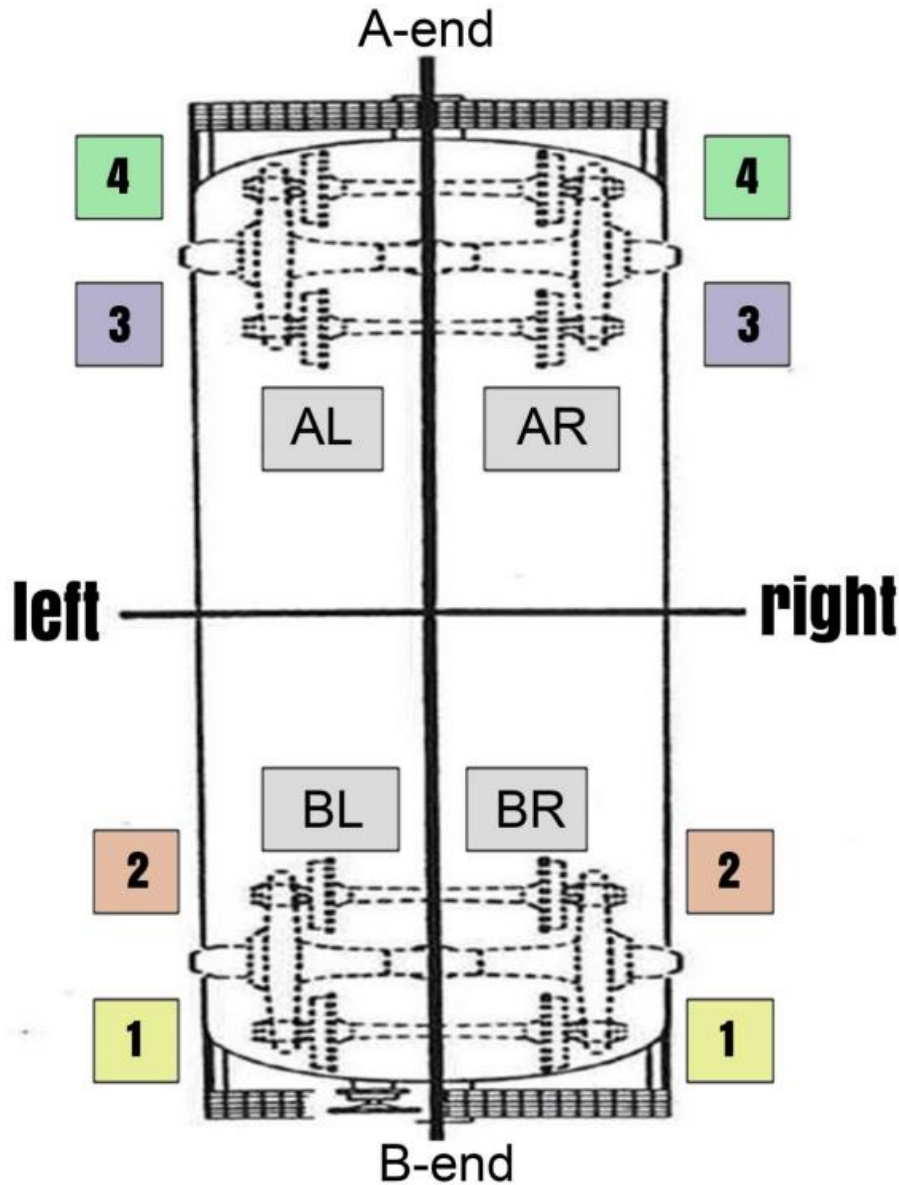
Figure 25 : AAR wheel-axle identification protocol

After two months of continuous data collection and monitoring, the wheel health index displayed some abnormalities which led to wheelset removals. HUM, in consultation with the owner of the railcars, requested the removal of the defective wheelset as indicated by the wheel health index data as well as two additional wheelsets with normal wheel health indexes for comparison. The axle removal procedure was documented, and pictures of this process are provided in Figure 26 and Figure 27. Two industrial size lift jacks were used to lift the railcar

and remove the corresponding axles for inspection. The bearings associated with these wheelsets were sent to the UTCRS bearing laboratory for systematic testing at speeds of 40 km/h (25 mph) and 64 km/h (40 mph) under empty and full railcar loads. The RMS and temperature data collected during the pilot field test for each bearing removed from service were then compared to the laboratory data acquired from running these bearings on the SBT. The purpose of this testing was to verify that the sensor data collected by the Boomerang for the same bearing was unaffected by field service operating conditions, which would imply that laboratory testing results of the Boomerang are transferable to rail service operation.

Figure 26: Field test wheelset removal process showing the industrial size lifting jacks used to

raise the railcar to release the wheelsets

Figure 27: A picture of the removed wheelsets

CHAPTER IV

EXPERIMENTAL RESULTS AND DISCUSSION

The Boomerang was evaluated by conducting a Level 1 root-mean-square (RMS) analysis on the data collected from several laboratory experiments and compared against the UTCRS wired and wireless sensor devices. The Boomerang and the UTCRS sensor modules were used to measure the vibration levels within the test bearing as quantified by the RMS values in g's. The acquired vibration profiles were then plotted along with the maximum and preliminary RMS thresholds. The preliminary threshold is established as an indicator for a possible defective bearing while the maximum threshold signifies a defective bearing. The Level 1 analysis is proof of functionality demonstrated by the Boomerang when the data measurements are within a ±1g RMS value as compared to the UTCRS sensor module results. The experimental results and discussion for each version of the Boomerang are explained in detail in this chapter.

4.1 Vibration testing of Boomerang A

The initial phase of testing performed utilizing Revision A of the Boomerang prototype focused on determining whether a defective bearing could be identified using this wireless system. The single bearing tester (SBT) was used throughout Experiment 228B to gauge the performance of Boomerang A. Based on the testing results, a failure root cause analysis (FRCA) was conducted to improve the Boomerang's design and mitigate issues found during testing.

In Experiment 228B, a defective bearing with a cone spall shown in Figure 20 was run on the SBT at a simulated train speed of 97 km/h (60 mph). The resulting vibration profiles of the bearing as captured by the Boomerang and the UTCRS wired and wireless devices are plotted in Figure 28. At an empty railcar load (i.e., 17% of full load), the RMS values for the Boomerang averaged 5.3g over the course of 2.7 hours of testing, while the reference wired accelerometer in the OB-SA location averaged an RMS value of 5.4g. Hence, the Boomerang RMS values were well within ±1g of the reference UTCRS wired accelerometer in the loaded zone (OB-SA). Once the bearing was subjected to 100% load (full railcar load equivalent to 153 kN per bearing), the OB-SA accelerometer exceeded the maximum threshold at 6g. Similarly, the Boomerang RMS increased to 7g correctly indicating a defective bearing. The RMS values at 100% applied load are representative of the increase in surface contact area between the cone spall and the rollers. Ultimately, the Boomerang was successfully in identifying the defective bearing.
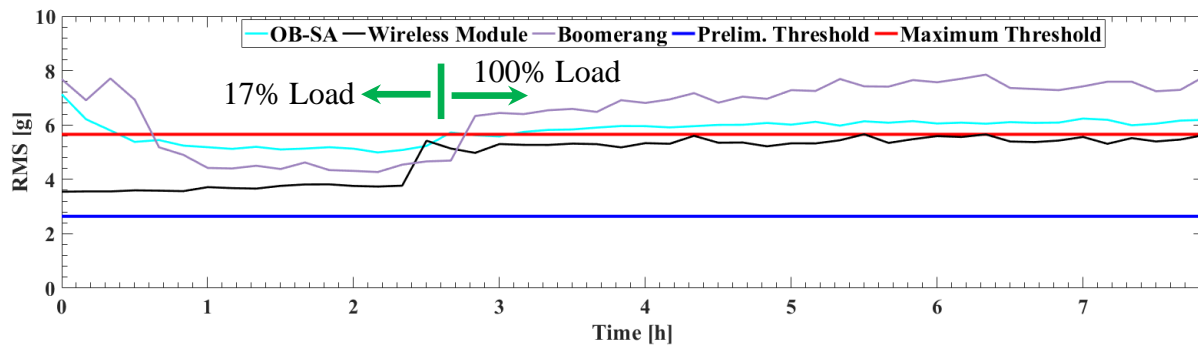
Figure 28: Experiment 228B vibration profiles for a bearing with a cone defect (spall) operating at 97 km/h (60 mph) under 17% and 100% railcar loads

As more tests were conducted, the Boomerang RMS values deviated well above the ±1g accuracy as compared to the reference UTCRS wired and wireless devices. The RMS data of a malfunctioning Boomerang are plotted in Figure 29 for a bearing operating at a simulated speed of 97 km/h under empty and full railcar loads.
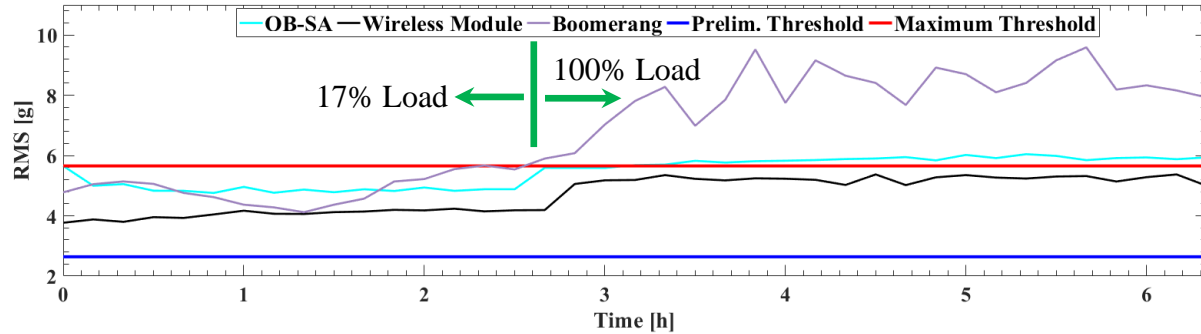
Figure 29: Vibration profile of a malfunctioning Boomerang acquired for a bearing with a cone spall running at 97 km/h (60 mph) under 17% and 100% applied loads

Looking at Figure 29, at empty railcar operating conditions (17% load), the mean RMS value for the Boomerang was 4.9g, which was within the ±1g accuracy when compared to the wired and the wireless module values of 4.8g and 4.1g, respectively. However, when the SBT load was increased from 17% to 100%, the mean RMS values for the wired and the wireless module increased to 6.0g and 5.2g, respectively, whereas the Boomerang vibration RMS became erratic and exhibited values that surpassed the ±1g accuracy with a good margin. The tendency for this erratic behavior was common when the Boomerang was exposed to high vibration levels.

After performing a failure root cause analysis, it was determined that the internal wires and components would malfunction due to unintended electrical contact caused by the excess vibration levels. Figure 30 displays the soldering sections that fractured and caused a short in the circuit, affecting the behavior of the accelerometer. Small fragments of Tin-Lead wire solder would be found between microprocessors and accelerometers when inspecting the Boomerang under a microscope.
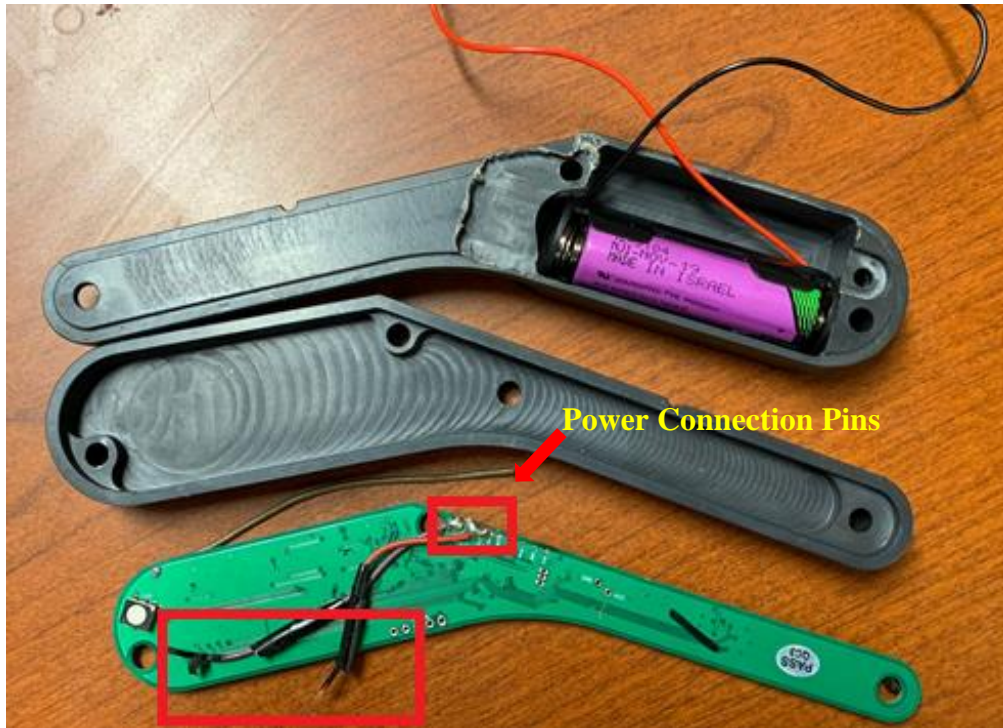
Figure 30: Boomerang A internal design showing the electrical wire junctions that would malfunction when exposed to excess vibration levels.

Another cause behind the abnormal behavior of Boomerang A was due to high temperature exposure over long periods of time. Revision A of the Boomerang was screwed directly onto the bearing adapter surface with the back side of the Boomerang making full contact with the adapter surface. At high operating speeds of 97 km/h or higher, the bearing operating temperature can reach upwards of 70°C (158°F), which leads the Boomerang to experience internal temperatures of 60°C (140°F) or more. Research has shown that accelerometer sensitivity deviation increases as temperature increases [33]. To reduce the temperature exposure, the Boomerang enclosure was modified to include rubber gaskets as demonstrated in Figure 31. The rubber gaskets insulate the Boomerang enclosure from direct surface contact with the adapter by providing a much needed air gap. This modification helped reduce the enclosure temperature down to 32°C (90°F).

Figure 31: Boomerang enclosure: (A) unmodified and (B) modified

To complete the FRCA, the circuit board was cleaned using isopropyl alcohol to remove any lingering debris, the solder joints were redone carefully using minimal Tin-Lead wire solder material, and the electrical wires were secured to mitigate excess motion when exposed to high vibration levels. Following these corrective measures, the Boomerang was affixed to the same bearing adapter and testing was resumed utilizing the same defective bearing with the cone spall operating at a simulated speed and load of 97 km/h and a full railcar load. The RMS results from this test are presented in Figure 32, which clearly indicate that the Boomerang RMS values are well within the $\pm 1g$ accuracy as compared to the wired (OB-SA) and wireless modules. Hence, the implemented Boomerang modifications successfully resolved the erratic behavior observed at high vibration levels.
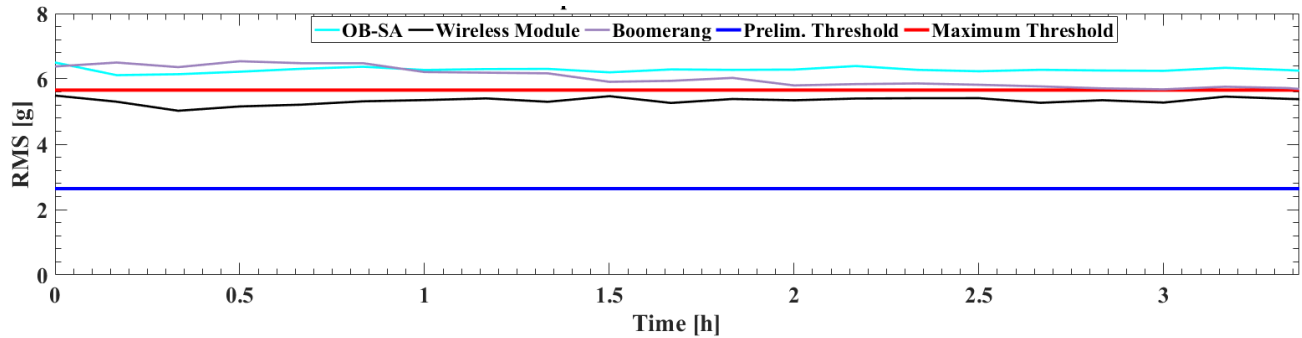
Figure 32: Vibration profiles for the defective bearing with the cone spall operating at 97 km/h (60 mph) under full railcar load acquired after implementing the Boomerang modifications based on the results of the failure root cause analysis

4.2 Boomerang B performance assessment and temperature correlation derivation

For the second revision of the Boomerang, Rev. B, an updated circuit board was designed and manufactured to include a temperature sensor and battery tabs as highlighted in Figure 33. A copper stud was soldered to the temperature sensor, as seen in the red frame, to measure the adapter temperature. The battery tabs in the yellow frame ensure a rigid connection with the batteries making wires obsolete. The four-bearing chamber tester (4BCT) and the single bearing tester (SBT) were utilized to obtain vibration signatures of healthy and defective tapered roller bearings. Additionally, the 4BCT was utilized to develop a bearing temperature correlation using a wide range of ambient temperatures, speeds, and railcar loads.
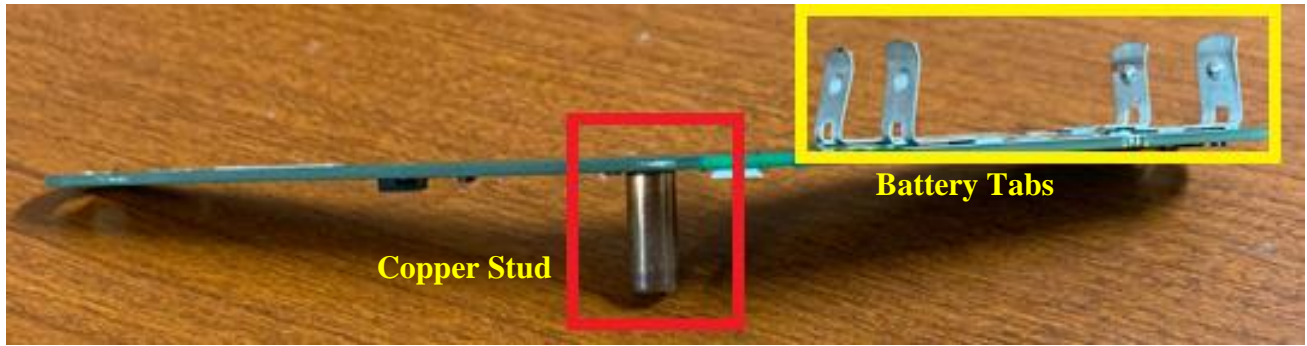
Figure 33: Boomerang B updated design: copper stud (left), battery tabs (right)

4.2.1 Verifying Accelerometer Functionality

Experiment 231, conducted on the four-bearing chamber tester (4BCT), tested a control class K bearing in the B2 position (refer to Figure 12) and a defective class K bearing with a cup (outer ring) spall in the B3 position. The control and the medium-sized cup spall are pictured in Figure 34 and Figure 35, respectively. The surface area of the cup spall is approximately 11.74 cm^2 (1.82 in^2).

Figure 34: Experiment 231 B2 - control bearing

Figure 35: Experiment 231 B3 – medium-size cup spall

Figure 36 presents the vibration profiles for the control bearing operating at 85 km/h (53 mph) and 100% load as acquired by the Boomerang and the UTCRS wired sensor (B2-SA). For five and a half hours of testing, the control bearing RMS values are slightly below the preliminary threshold for both the Boomerang and the wired device. The Boomerang reported an average RMS value of 2.2g, while the B2-SA wired accelerometer measured an average RMS value of 1.9g. The close agreement between the RMS values as measured by the Boomerang and the wired device verifies the functionally of the second revision of the Boomerang (i.e., Rev. B).
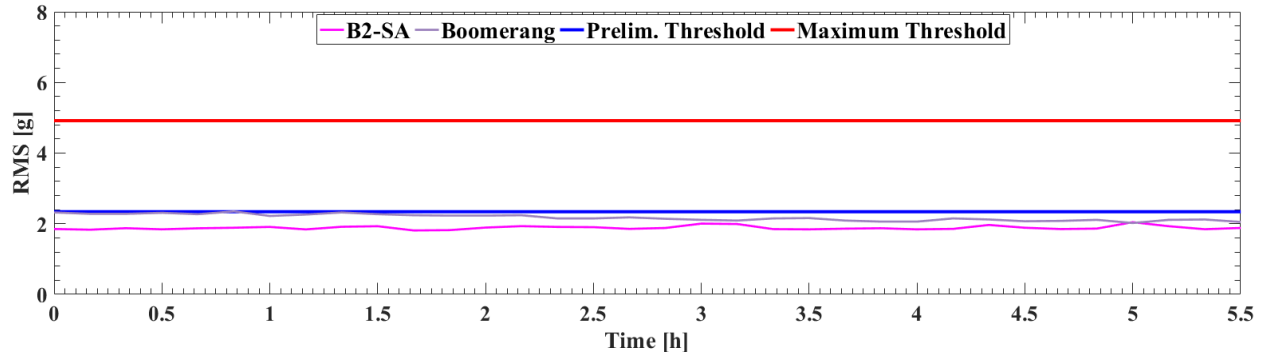
Figure 36: Experiment 231, Boomerang B vibration profile for control bearing B2 operating at 85 km/h (53 mph) under 100% applied load (fully loaded railcar)

Simultaneously, a second Boomerang affixed to the adapter of the defective bearing with the cup spall monitored and recorded the vibration levels within that bearing. The vibration profile of the defective bearing is given in Figure 37. The Boomerang and B3-SA wired accelerometer averaged RMS values of 4.8g and 5.3g, respectively. With this marginal difference in RMS values between the two systems (i.e., 0.5g), the fidelity of the Boomerang was confirmed. Since the Boomerang RMS value was at or above the maximum threshold indicated by the horizontal red line in Figure 37, that denoted the presence of a defect within that bearing which was an accurate assessment given that the bearing had a cup spall.
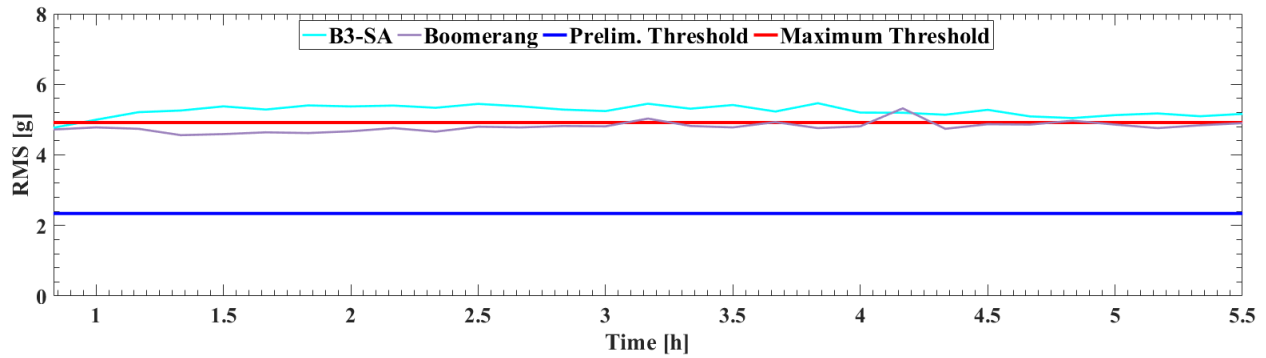
Figure 37: Experiment 231, Boomerang B vibration profile for defective (cup spall) bearing B3 operating at 85 km/h (53 mph) under 100% applied load (fully loaded railcar)

Additional testing of Boomerang B was carried out on the SBT with a bearing containing a large cup spall with a defect size of 50.65 cm^2 (7.85 in^2) as depicted in Figure 38. Experiment 232 was conducted at 17% railcar load and a simulated train speed of 85 km/h (53 mph) for a test duration of 1.6 hours.

Figure 38: Large cup (outer ring) spall used in Experiment 232 for validation testing of Boomerang B

At a simulated empty railcar load (i.e., 17% load) and a speed of 85 km/h (53 mph), the

Boomerang Rev. B, the wired device, and the wireless module had mean RMS values of 8.4g,

8.4g, and 8.3g, respectively. After 1.6 hours of testing at the 17% load conditions, the applied

load was increased to 100% simulating a fully loaded railcar. At 100% railcar load, the

Boomerang, the wired system, and the wireless module had mean RMS values of 13.2g, 14.2g,

and 13.8g, respectively. All three systems indicated a severely defective bearing above the

maximum threshold, once again validating the functionality and reliability of the Boomerang B.
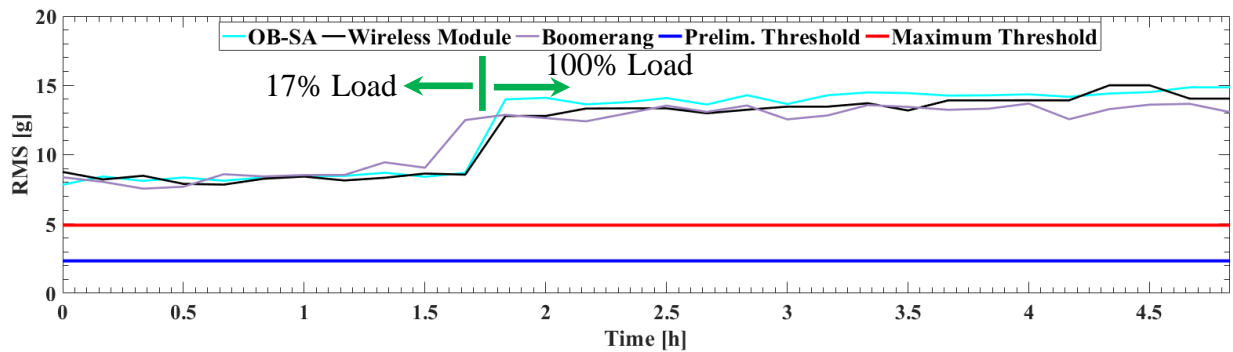
Figure 39: Experiment 232, Boomerang B vibration profile for a defective (cup spall) bearing

operating at 85 km/h (53 mph) under 17% (empty railcar) and 100% (fully loaded railcar)

applied loads

4.2.2 Boomerang Temperature Transfer Function

A polynomial regression model was developed by systematically comparing the recorded

Boomerang temperature data measured by the copper stud to the corresponding bearing

operating temperatures read by the wired thermocouples. The resulting correlation provides a

temperature transfer function that can be used to accurately predict the bearing operating

temperature from the Boomerang temperature measurement taken at the adapter surface by the

contacting copper stud. The temperature data collected from the experiments involving the 4BCT

is presented in Figure 40. These datasets were acquired from numerous laboratory experiments

carried out on various Class F and Class K bearings, both healthy and defective, with defect

areas ranging from small (< 6.45 cm^2 or 1 in^2) to large (> 12.9 cm^2 or 2 in^2). The bearings were

tested at empty and full railcar loads with operating speeds ranging from 40 km/h (25 mph) to

137 km/h (85 mph). These datasets also included bearing operating temperatures recorded with

the 4BCT set to run at ambient conditions as low as -20°C (-4°F) and up to 26°C (79°F). The

main goal of this cold ambient testing was to ensure that the low temperatures did not affect the

functionality or accuracy of the Boomerang temperature sensor, especially as it concerns the

copper stud thermal contraction effects.
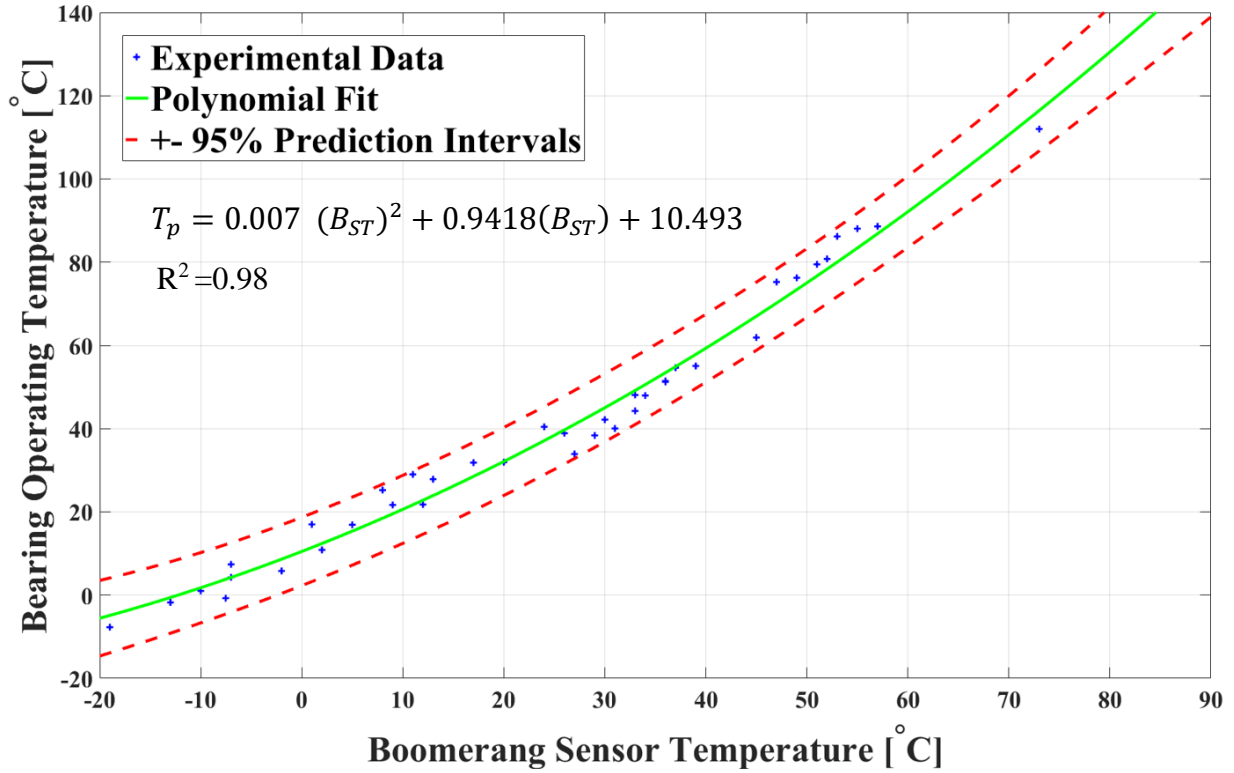
Figure 40: Second-order polynomial regression fit correlating the acquired adapter surface temperature (B_{st}) to the bearing operating temperature (T_p) Also shown are the 95% confidence intervals

$$T_p = 0.007 \ (B_{ST})^2 + 0.9418(B_{ST}) + 10.493 \qquad (1)$$

Equation (1) gives the second-order regression model that was derived from the data presented in Figure 40. Equation (1) has a goodness-of-fit (R^2) value of 98% indicating that the recorded Boomerang sensor temperature readings (B_{ST}) can accurately predict the bearing operating temperature (T_p) utilizing this transfer function. Table 3 provides a representative sample of the data used to develop the regression model, which includes the temperature difference as a measure of error after applying the temperature correlation.

Table 3: Actual bearing operating temperature versus predicted bearing operating temperature along with the temperature difference in the prediction. This sample dataset was acquired at an ambient temperature of 22°C (72°F)

Acquired Boomerang Temperature [°C]	Predicted Bearing Operating Temperature [°C]	Actual Bearing Operating Temperature [°C]	Absolute Temperature Difference [°C]
31	46	40	6
33	49	44	5
36	53	51	2
37	55	55	0
49	73	76	3
52	78	81	3
57	87	89	2
27	41	34	7
29	44	38	6
30	45	42	3
34	51	48	3
36	53	51	2
39	58	55	3
45	67	62	5

A maximum temperature difference of 8°C (14°F) was found between the actual bearing operating temperature, measured directly by thermocouples, and the predicted bearing operating temperature, generated by the devised regression model. Note that all predicted values were within the 95% confidence interval and, in general, the predicted values overestimated the actual bearing operating temperatures, which implies that no overheated bearings will go undetected.

Finally, it is important to remind the reader that the Boomerang temperature transfer function is subject to continuous improvement as more experiments are performed resulting in more data

being added to the complete dataset that generates the correlation. A complete table with the temperature data used to derive the correlation of Equation (1) can be found in Appendix A.

4.3 Boomerang C Performance Assessment

After proving the functionality of Boomerang B, the third revision of the Boomerang (Rev. C) implemented an additional 200g three-axes accelerometer and utilized the preliminary temperature correlation derived using Rev. B Boomerang. The performance of Boomerang C was investigated in Experiments 233 and 232B.

Experiment 233 evaluated Boomerang C on the 4BCT utilizing Class F bearings with the B2 position occupied by a control (defect-free) bearing and the B3 position occupied by a defective bearing with a cone spall, shown in Figure 41. The cone spall area was approximately 8.90 cm^2 (1.38 in^2).

Figure 41: Experiment 233 cone defect tested in B3 position

Figure 42 displays the average RMS values reported by the Boomerang and wired module (B2-SA) for the healthy (control) bearing over the long duration test of 90 hours. Operating at 85 km/h (53 mph) and 100% applied load, the RMS values averaged 3.0g for the Boomerang and 2.5g for the B2-SA accelerometer. The Boomerang performed as expected closely matching the RMS values of the wired reference accelerometer (within 0.5g), and both devices indicated a defect-free bearing since the RMS values were at or slightly above the preliminary threshold but well below the maximum threshold. The reader is reminded that RMS values above the maximum threshold signify a defective bearing with a very high confidence level.
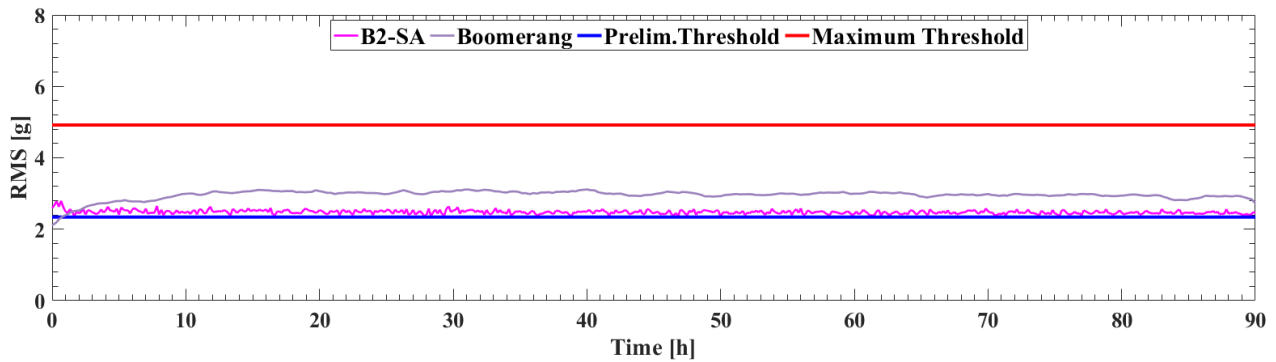
Figure 42: Experiment 233, vibration profiles for control bearing B2 operating at 85 km/h (53 mph) under 100% applied load (fully loaded railcar)

Note that the bearing operating temperatures presented in the figures of this thesis are not the absolute temperatures but rather the temperatures above ambient conditions. Hence, the temperature difference (ΔT) is the difference between the absolute bearing operating temperature and ambient temperature. In the case of the defect-free (control) bearing, the predicted steady state bearing operating temperature (T_p) acquired by the Boomerang through the correlation of Equation (1) was 32°C (58°F) above ambient conditions, as can be seen in Figure 43. The actual steady state bearing operating temperature as calculated from the average of the three K-type

thermocouples (one regular and two bayonet style) was 31°C (56°F) above ambient conditions. Thus, the results demonstrate that temperatures read by the Boomerang, B2 thermocouple, and B2 Bayonet were all within 1°C (2°F), which validates both the functionality of the Boomerang temperature sensor and the accuracy and reliability of the devised temperature transfer function.
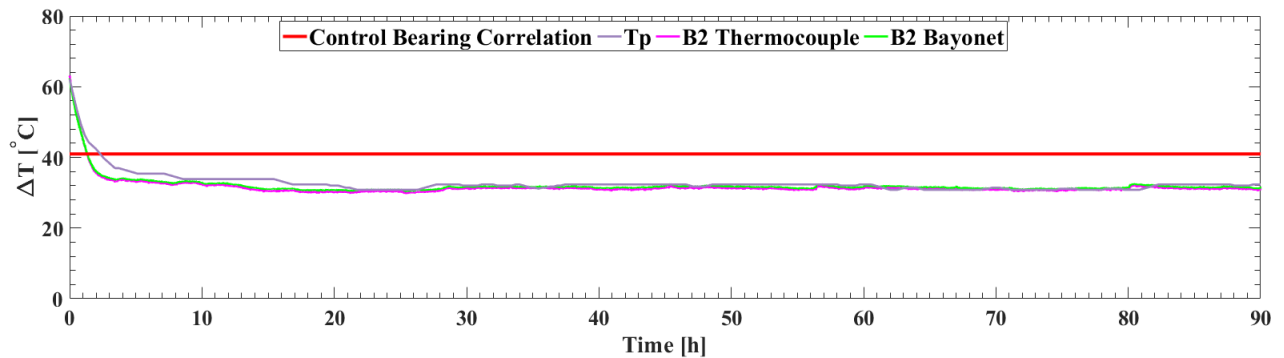
Figure 43: Experiment 233, temperature profiles for control bearing B2 operating at 85 km/h (53 mph) under 100% applied load (full railcar) [ambient temperature was 22°C or 72°F]

The vibration profiles of the defective bearing with the cone spall are shown in Figure 44. Throughout the 90-hour test, both the Boomerang and the wired (B3-SA) accelerometers exhibited RMS values that were at or above the maximum threshold that normally signifies a defective bearing. The average RMS values for the Boomerang and the wired device were 5.4g and 4.7g, respectively. It is apparent that the Boomerang successfully identified the defective bearing, thus providing further validation of its functionality.
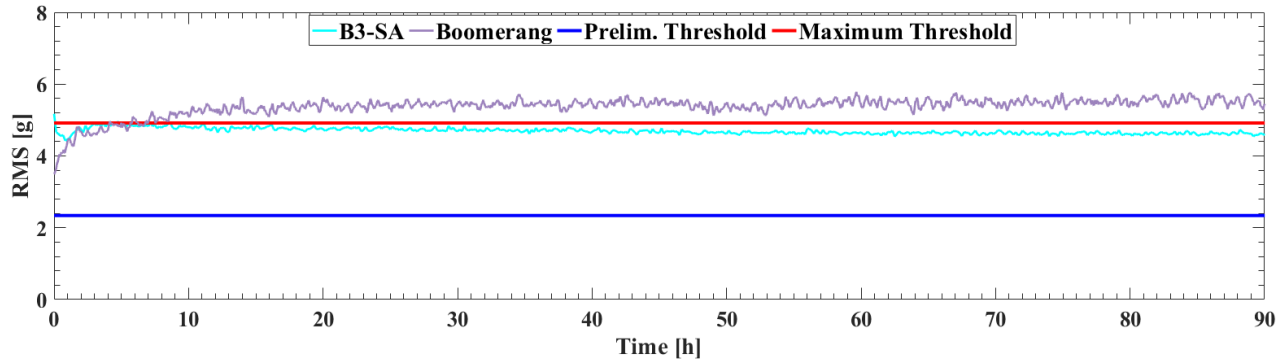
Figure 44: Experiment 233, vibration profiles for the defective (cone spall) bearing B3 operating

at 85 km/h (53 mph) under 100% applied load (fully loaded railcar)

Looking at Figure 45, it appears that the Boomerang affixed to the defective bearing in

the B3 location also yielded accurate results in terms of the predicted bearing operating

temperature. The average predicted bearing operating temperature acquired by the Boomerang

was 27°C (49°F) above ambient conditions while the wired thermocouples measured an average

bearing operating temperature of 26°C (47°F) above ambient conditions. Again, the difference in

the two readings was a mere 1°C. Interestingly, when comparing the bearing operating

temperatures of the control (healthy) and the defective bearing, one can notice that the defective

bearing ran cooler than the healthy bearing. This observation further supports the findings

published in earlier works which suggest that vibration signatures are a much better indicator of

bearing health than temperature profiles. The data presented here validates those claims.
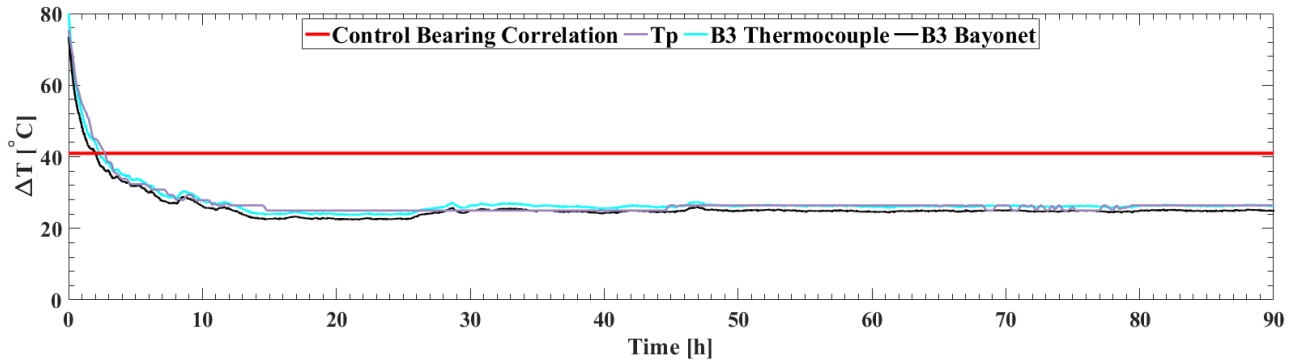
Figure 45: Experiment 233, temperature profiles for defective (cone spall) bearing B3 operating at 85 km/h (53 mph) under 100% applied load [ambient temperature was 22°C or 72°F]

The purpose of Experiment 232B was to evaluate the Boomerang performance under several speed and load conditions using the defective bearing with the severe cup spall pictured in Figure 38. The RMS values for the Boomerang were compared to the reference wired and wireless sensor modules at several instants throughout the experiment. Table 4 provides a summary of the acquired RMS values for the large cup spall under different operating conditions.

Table 4: Experiment 232B RMS comparison between the Boomerang and the UTCRS Condition Monitoring Devices

Railcar load	Speed [km/h]	Maximum Threshold [g]	HUM Boomerang [g]	UTCRS Wired [g]	UTCRS Wireless [g]
17% (Empty railcar)	40	1.6	2.3	2.4	2.2
	64	3.2	6.1	5.2	7.2
	85	4.6	10.5	9.0	11.7
100% (Fully loaded railcar)	40	1.6	2.6	2.3	2.8
	64	3.2	6.5	7.0	7.4
	85	4.6	11.9	12.2	10.3

The Boomerang was evaluated to see if the RMS readings were within ±1g of the reference monitoring devices. At 17% railcar load, the Boomerang and the wired RMS values were within ±1g at 40 km/h and 64 km/h. The RMS values between the Boomerang and the wired device differed by 1.5g while operating at a speed of 85 km/h (53 mph). At empty railcar loads and high speeds, the vibration levels within the bearing vary as the lower applied loads allow the inner components of the bearing to vibrate freely leading to more frequent roller misalignments. Moreover, the UTCRS wired device is equipped with a 16th order elliptical filter that cuts off high frequency noise, whereas the Boomerang and the UTCRS wireless device do not have that filter. For these two reasons, the Boomerang RMS value is 1.5g above that of the wired device at these operating conditions. Nevertheless, since all three condition monitoring devices report RMS values that are well above the maximum threshold, the railcar owner will be alerted of the presence of a defective bearing even at an empty railcar load.

For a fully loaded railcar (100% load), the RMS values for the Boomerang and the wired device were within ±1g. Note that, at full load, the surface contact between the rollers and the spalled region increases, which results in slightly higher RMS values, as seen in Table 4. Also, an increase in the operational speed led to a rise in the RMS values reported by the Boomerang and the UTCRS monitoring devices. In conclusion, the Boomerang reported RMS values that were above the maximum threshold under all tested operating conditions, thus correctly identifying the defective bearing.

Finally, Table 5 summarizes the predicted bearing operating temperatures measured by the Boomerang as compared to the actual bearing operating temperatures recorded by the thermocouples at empty and full railcar loads and speeds of 40 km/h (25 mph), 64 km/h (40 mph), and 85 km/h (53 mph).

Table 5 : Experiment 232B Boomerang temperature verification data summary

Railcar load	Speed [km/h]	Actual Bearing Operating Temperature [°C]	Predicted Bearing Operating Temperature [°C]	Temperature Difference [°C]
17% (Empty railcar)	40	33	34	1
	64	33	29	4
	85	33	33	0
100% (Fully loaded railcar)	40	39	35	4
	64	49	43	6
	85	53	49	4

As mentioned in the temperature correlation section of this thesis, the maximum temperature difference observed was 8°C (14°F) regardless of the bearing class (F or K), operating speed and load, or condition. For Experiment 232B, the largest temperature difference between the predicted bearing operating temperature and the actual bearing operating temperature was 6°C (11°F) at 64 km/h (40 mph) and 100% load.

CHAPTER V

FIELD TEST RESULTS

A pilot test was carried out to assess the readiness of the Boomerang for rail service implementation. Figure 46 is a picture of the forty Boomerangs and five Gateways that were installed on nine different privately owned railcars.

Figure 46: Assembled Boomerangs and Gateways used for field test implementation

After monitoring the data reported by the Boomerangs, three wheelsets were scheduled for removal based on their wheel health index profiles. Note that the wheel health index is the subject of a parallel study that is assessing the Boomerang functionality as a wheel condition monitoring device. As previously mentioned, Boomerang C (Rev. C) was equipped with a 200g

three-axes accelerometer that was used for wheel impact detection. Interestingly, the forty Boomerangs deployed reported healthy bearings during the pilot test, but two Boomerangs indicated a bad wheelset through the wheel health index criteria. Therefore, HUM in consultation with the railcar owner decided to remove the bad wheelset along with two other healthy wheelsets for validation testing to be performed at the UTCRS bearing laboratory.

Operating with normal wheel health indexes, Figure 47 displays wheelset 1 removed from service with L2 and R2 wheel indicators. The bearings associated with the three removed wheelsets were sent to the UTCRS laboratory for systematic testing at speeds of 40 km/h (25 mph) and 64 km/h (40 mph) under empty and full railcar loads. These two speeds were specifically chosen because these railcars operate at these speeds for most of their trips. The RMS and temperature data collected during the field test for each bearing from wheelset 1 were compared to the laboratory data acquired from operating these bearings on the single bearing tester (SBT). Table 6 and Table 7 present the RMS and absolute temperature data acquired from the field and laboratory tests for bearing R2 of wheelset 1.

Figure 47: Field wheelset 1 with L2 and R2 wheel identifiers

Table 6: Wheelset 1, bearing R2 laboratory and field RMS summary

Railcar load	Speed [km/h]	Maximum Threshold [g]	Laboratory Boomerang [g]	Field Boomerang [g]
17% (Empty railcar)	40	1.6	0.9	1.0
	64	3.2	0.8	1.2
100% (Fully loaded railcar)	40	1.6	1.3	1.2
	64	3.2	1.1	1.5

Table 6 provides a summary of the field and laboratory mean RMS values at speeds of 40 km/h and 64 km/h under empty and fully loaded railcar conditions for wheelset 1 R2 bearing. The results show that the R2 bearing is classified as healthy since the RMS values remain below the maximum threshold for the common railcar speeds and railcar loads. The laboratory and field RMS values are within 0.5g of each other which confirms the effectiveness of the Boomerang in both field and laboratory conditions.

The absolute wheelset 1 R2 bearing operating temperatures for the laboratory and field tests are shown in Table 7. These results validate previous laboratory results obtained while developing the Boomerang temperature correlation (transfer function) which stated a maximum temperature difference of 8°C (14°F). It is important to note that the data collected in the field by the Boomerang was done on an hourly basis and, therefore, the acquired Boomerang temperatures in the field may not have been taken during steady state operation. In contrast, the Boomerang temperature data recorded in the laboratory are all steady-state temperatures taken at the operating speed and load conditions. The latter can easily explain the 8°C temperature difference seen at an empty railcar load and a speed of 64 km/h. If, at the time the Boomerang took the temperature data, the railcar had just reached a speed of 64 km/h, the temperature lag

associated with the bearing not reaching steady-state operation can be responsible for the 8°C lower bearing operating temperature measured in the pilot field test. Regardless, the data presented in Table 7 demonstrates the functionality of the Boomerang and validates the accuracy and reliability of the temperature transfer function for rail service applications.

Table 7: Wheelset 1, bearing R2 absolute laboratory and field temperature comparison

Railcar load	Speed [km/h]	Laboratory Predicted Bearing Operating Temperature [°C]	Field Predicted Bearing Operating Temperature [°C]	Temperature Difference [°C]
17% (Empty railcar)	40	39	40	1
	64	49	41	8
100% (Fully loaded railcar)	40	48	46	2
	64	55	51	4

Table 8 gives a complete summary of the RMS values recorded for the wheelset 1 L2 bearing. Following the same systematic testing at speeds of 40 km/h (25 mph) and 64 km/h (40 mph) under empty and full railcar loads, bearing L2 for wheelset 1 exhibited RMS values below the maximum threshold indicating a healthy bearing. The RMS value of bearing L2 during the pilot field test at operating conditions of 40 km/h under full load was slightly above the maximum threshold but within the ±1g margin of error associated with this accelerometer. Moreover, when the operating speed increased to 64 km/h, the RMS values settled below the maximum threshold confirming the condition of the bearing as healthy. The laboratory and field RMS values matched within 0.6g indicating a functioning Boomerang system in both field and laboratory conditions.

Table 8: Wheelset 1, bearing L2 laboratory and field RMS summary

Railcar load	Speed [km/h]	Maximum Threshold [g]	Laboratory Boomerang [g]	Field Boomerang [g]
17% (Empty railcar)	40	1.6	1.0	1.1
	64	3.2	0.9	1.4
100% (Fully loaded railcar)	40	1.6	1.5	2.1
	64	3.2	1.2	1.7

Table 9 lists the laboratory and field L2 bearing operating temperatures. At 40 km/h and 64 km/h under both empty and full railcar load conditions, the predicted bearing operating temperatures are within 5°C or less in both laboratory and field operation.

Table 9: Wheelset 1, bearing L2 absolute laboratory and field temperature comparison

Railcar load	Speed [km/h]	Laboratory Predicted Bearing Operating Temperature [°C]	Field Predicted Bearing Operating Temperature [°C]	Temperature Difference [°C]
17% (Empty railcar)	40	40	40	0
	64	46	44	2
100% (Fully loaded railcar)	40	44	46	2
	64	47	52	5

CHAPTER VI

CONCLUSIONS

The University Transportation Center for Railway Safety (UTCRS) partnered with Hum Industrial Technology Inc. (HUM) to develop a wireless onboard condition monitoring system called the Boomerang™. The Boomerang utilizes accelerometers and temperature sensors to assess the health of a tapered roller bearings deployed in the rail industry. The results presented in this thesis validate the functionality of the Boomerang under different speed and load conditions that replicate rail service operation. The UTCRS wired and wireless modules were directly compared against the Boomerang to gauge its performance. The Boomerang was comprehensively tested in both laboratory and field scenarios to assess the accuracy and reliability of the data collected by the Boomerang's temperature and vibration sensors.

Using the Level 1 RMS analysis developed by the UTCRS, bearings containing a defect in the outer ring (cup) or inner ring (cone), with varying defect areas, were analyzed using two UTCRS bearing test rigs with bearing adapters housing the onboard condition monitoring systems. Although the first revision of the Boomerang (Rev. A) produced favorable results for the most part, the readings varied due to faulty contacts and overheating electrical components. After conducting a failure root cause analysis (FRCA), the circuit board was redesigned along with modifications to the Boomerang enclosure. These improvements allowed for favorable results within ±1g in RMS values.

In the second revision of the Boomerang (Rev. B), the vibration profiles were reevaluated to determine the accuracy of the redesigned circuit board. After successfully detecting two defective bearings using the Level 1 RMS analysis, the thresholds set by UTCRS did not need adjustments to detect defective bearings. With the integration of a temperature sensor within the Boomerang, temperature-related issues in bearings can be closely monitored. By developing an accurate temperature correlation (transfer function) between the bearing operating temperature and Boomerang temperature sensor reading, the Boomerang temperature can be used to predict the actual bearing operating temperature within ±8°C (14°F). The developed second-order polynomial regression temperature correlation has a 98% goodness-of-fit (R^2) value through temperatures ranging from -20°C (-4°F) to 100°C (212°F).

For the third revision of the Boomerang (Rev. C), a final assessment of vibration and temperature signatures was completed prior to a pilot test deployment. The vibration signatures for a 90-hour duration test averaged RMS values within the tolerance of ±1g between the Boomerang and the UTCRS devices (used as reference) while testing a control and a defective bearing. The predicted temperatures from the Boomerang utilizing the second-order polynomial correlation were within 1°C of the actual bearing operating temperatures at all tested operating conditions. The Boomerang was also tested for instantaneous RMS values on the single bearing tester (SBT) at varying speeds and railcar loads for a defective bearing with a severe cup spall. The Boomerang identified the severely defective bearing by reporting RMS values that were above the maximum RMS thresholds at all operating conditions tested.

After completing the performance assessment of the Boomerang, forty Boomerangs were assembled for a pilot test and monitored continuously for two months. After analyzing the data collected from the forty Boomerangs, three wheelsets were schedule for removal based on wheel

health indexes. To demonstrate the efficacy of the Boomerang, a control wheelset was removed and had the corresponding bearings tested on the UTCRS SBT. After compiling the field and laboratory RMS values for the corresponding bearings, a maximum RMS difference of ±0.6g was measured between field and laboratory conditions. The Boomerang also measured the bearing operating temperatures to within ±8℃. The results for both field and laboratory testing demonstrated that the Boomerang functions as intended with an acceptable level of efficacy being unaffected by the harsh operating conditions of the freight rail service.

Overall, the validation of the new HUM onboard monitoring system was declared a success. The Boomerang™ is a new wireless onboard condition monitoring system deemed ready for field implementation based on the results and discussions provided throughout this study. Being an onboard device, the Boomerang can improve railway safety by providing a proactive solution for rolling stock maintenance scheduling, thus mitigating unnecessary and costly train stoppages and delays and eliminating catastrophic rolling-stock-related derailments or accidents.

REFERENCES

[1]   The Beginnings of American Railroads and Mapping. Sep. 2021
        https://www.loc.gov/collections/railroad-maps-1828-to-1900/articles-and-essays/history-
        of-railroads-and-maps/the-beginnings-of-american-railroads-and-mapping/

[2]   Federal Railroad Administration, Railroad Safety, August. 2021
        https://railroads.dot.gov/railroad-safety

[3]   Association of American Railroads, "A short History of U.S. Freight Railroads
        Newsletter", April 2021 https://www.aar.org/wp-content/uploads/2020/08/AAR-
        Railroad-Short-History-Fact-Sheet.pdfdf

[4]   3.10 – Accident Causes | Federal Railroad Administration, Office of Safety Analysis,
        Web Accessed Sep 7, 2021. https://safetydata.fra.dot.gov/OfficeofSafety/default.aspx

[5]   S. Bert, C. Keller, O. Parsons, M. Randall, J. Poslusny, P. Ashtankar, A. Lahare, M.
        Salunke, S. Searcy, D. Findley, "Comprehensive Cost of Rail Incidents in North
        Carolina", ITRE, Dec. 2020.

[6]   Progressiverailroading, "When a train derails, many railroads turn to contractors to
        contain and clean up spills", August 2006,
        https://www.progressiverailroading.com/mow/article/When-a-train-derails-many-
        railroads-turn-to-contractors-to-contain-and-clean-up-spills--13396

[7]   Association of American Railroads, "Freight Rail Technology" Web Accessed Sep 9,
        2021, https://www.aar.org/topic/freight-rail-tech

[8]   "Railway Bearings | Railway Bearings in India - NBC Bearings Jaipur."
        https://www.nbcbearings.com/railway-Products.php

[9]   Freight Rail Works, Association of American Railroads, "Nationwide Wayside Detector
        System", Web Accessed Sep 10, 2021, www.freightrailworks.org, www.aar.org.

[10]   T. Sultana, "Safety Impact of Wayside Detector Systems, Systems, Improved Automated Equipment Inspection," in 22nd Annual AAR Reserach Review, Pueblo, CO, 2017

[11]   United States, Department of Transportation & Federal Railroad Administration. "An Implementation Guide for Wayside Detector Systems" May 2019

[12]   C. Tarawneh, J. Aranda, V. Hernandez, S. Crown & J. Montalvo (2020) "An investigation into wayside hot-box detector efficacy and optimization," International Journal of Rail Transportation, 8:3, 264-284, DOI: 10.1080/23248378.2019.1636721

[13]   Tarawneh, C., Ph,D., Sotelo, L., Villarreal, A., De Los Santos, N., Lechtenberg, R., Jones, R., "Temperature Profiles of Railroad Tapered Roller Bearings with Defective Inner and Outer Rings." Proceedings of the 2016 Joint Rail Conference, April 12-15, 2016, Columbia, SC, USA

[14]   Tarawneh, C., Ph.D., et al., "Experiments and Model for the Thermal Response of Railroad Tapered-Roller Bearings." International Journal of Heat and Mass Transfer, 2008. 51: p. 5794-5803

[15]   A. Gonzalez," Development, optimization, and implementation of a vibration-based defect detection algorithm for railroad bearings," Master's Thesis, University of Texas Rio Grande Valley, May 2015

[16]   Amstrong, John and Kluge, Frank C.Overheated Journal Bearing Derailment Prevention System. 3,930,629 United States of America, January 6, 1976.

[17]   Ronald R. Newman, R.C.L., John Tabacchi, David Purta, Hot Bearing Detection with the "Smart-BoltTM", in ASME/IEEE Joint Railroad Conference, 1990: Chicago, IL pp 105-110

[18]   Bowser, "Blue bearing caps." Sep 1, 2016. Web accessed: Sep 12, 2021. https://www.trains.com/trn/train-basics/ask-trains/blue-bearing-caps/

[19]   Science Direct, "Sensor Node," LPWAN Technologies for IoT and M2M Applications, 2020 https://www.sciencedirect.com/topics/engineering/sensor-node/pdf

[20]   M. French, K. Iftekharuddin, D. Leeper, R. Samy, W. Hwang, "BEARING WITH WIRELESS SELF-POWERED SENSOR UNIT," United States Patent, Mar 18, 2003.

[21]   The Modal Shop an Amphennol Company, "How Temperature Affects Accelerometer Calibration," web accessed Sep 14, 2021. https://www.modalshop.com/calibration/.asp?ID=785

[22]   B. Wilson, A. Martin, "Bearing Condition Monitoring Using Wireless Technology to Reduce the Risk of Bearing Failure," Proceedings of the ASME 2012 Rail Transportation Division Fall Technical Conference, Oct 16-17, 2012, Omaha, Nebraska, USA

[23]   A. Zagours II, "Implementation of Wireless Temperature Sensors for Continuous Condition Monitoring of Railroad Bearings" Master's Thesis, Department of Mechanical Engineering, The University of Texas Pan-American, May 2012

[24]   Railway Technology, "IONX Asset Monitoring", web accessed Sep 12, 2021. https://www.railway-technology.com/contractors/vehicle/ionx

[25]   Amsted Digital Solutions, "Technology" web accessed Sep 12, 2021. https://www.amsteddigital.com/technology/

[26]   J. Montalvo, " Defect detection algorithm optimization for use in freight railcar service," Master's Thesis, Department of Mechanical Engineering, The University of Texas Rio Grande Valley, August 2019

[27]   C. Tarawneh, J. Montalvo, B. Wilson, "Defect Detection in freight railcar tapered-roller bearings using vibration techniques," Rail. Eng. Science, August 31, 2020.

[28]   J. Cuanang, "Optimizing a Railroad Bearing Condition-Monitoring Algorithm for use with an Onboard Wireless Low-Power Sensor Module," Master's Thesis, Department of Mechanical Engineering, The University of Texas Rio Grande Valley, December 2020

[29]   Parsons, "Keeping a Pulse on Rail," RailpulseTM, 2021 Parsons Corporation, web accessed Sep 12, 2021. https://www.parsons.com/products/railpulse/

[30]   Association of American Railroads, "Freight Railroads & Positive Train Control," fact sheet, web accessed Sep 10, 2021. https://www.aar.org/campaigns/ptc/#!

[31]   Progressive RAILROADING, "Data Analytics is giving rail asset owners new ways to improve their predictive maintenance practices," Rail News Home, Internet Digital, May 2019. Web accessed August 2021. https://www.progressiverailroading.com/internet-digital/article/Data-analytics-is-giving-rail-asset-owners-new-ways-to-improve-their-predictive-maintenance-practices--57544

[32]   Hum Industrial Technology, Web Accessed March 2, 2020 https://www.humindustrial.com/

[33]   G. Ruzza, L. Guerriero, P. Revellino, F. Guadagno, " Thermal Compensation of Low-Cost MEMS Accelerometers for tilt Measurements." MFPI sensors, August 2018

APPENDIX A

APPENDIX A

TEMPERATURE CORRELATION

Table A.1: Temperature readings for a class K cone defective bearing operating at 72 km/h (45mph) with a 21°C ambient temperature

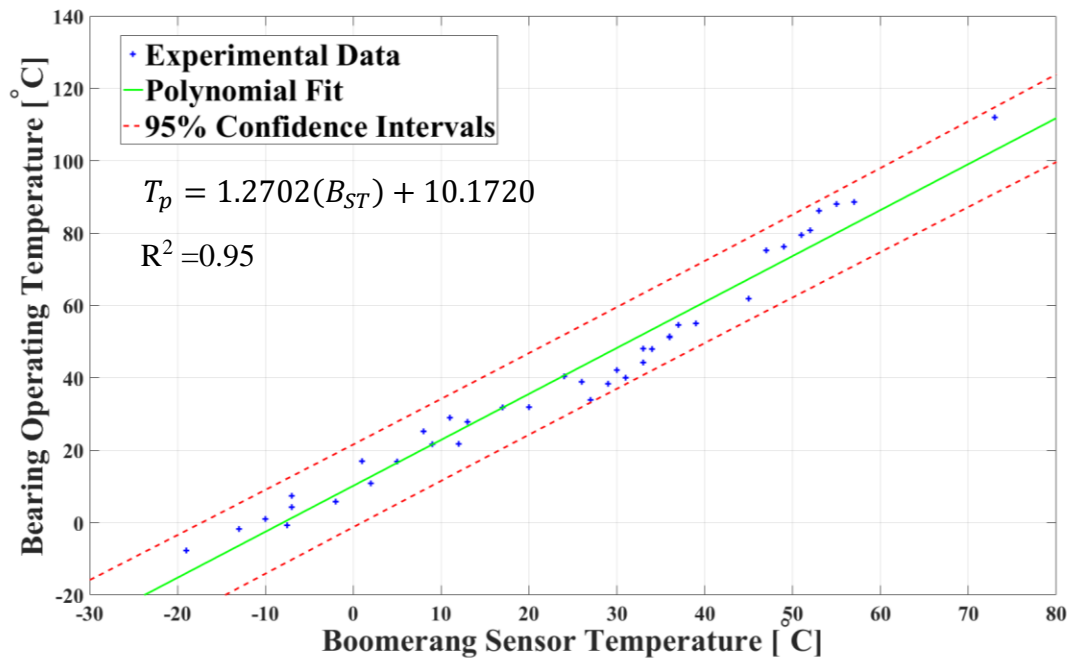| Readings	Boomerang Temperature [°C]	Average Thermocouple and Bayonets Temperature [°C]
1	30	42
2	30	42
3	30	42
4	30	42
5	30	42
6	30	42
7	30	42
8	30	42
9	30	42
10	30	42
11	30	42
12	30	42
13	30	42
14	30	42
15	30	42
16	30	42
17	30	42
18	30	42
19	30	42
20	30	42
21	30	42
22	30	42
23	30	42
24	30	42
25	30	42
26	30	42
27	30	42
28	30	42
29	30	42
30	30	42
Average	30	42

Figure A 1: First-order polynomial regression fit correlating the acquired adapter surface temperature (B_{st}) to the bearing operating temperature (T_p) Also shown are the 95% confidence intervals

Table A.2 : Actual Bearing Operating Temperature vs. Predicted Bearing Operating Temperature (Complete Data Set)

Acquired Boomerang Temperature [°C]	Predicted Bearing Operating Temperature [°C]	Actual Bearing Operating Temperature [°C]	Absolute Temperature Difference [°C]
31	46	40	6
33	49	44	5
36	53	51	2
37	55	55	0
49	73	76	3
52	78	81	3
57	87	89	2
27	41	34	7
29	44	38	6
30	45	42	3
34	51	48	3
36	53	51	2
39	58	55	3
45	67	62	5
-19	-5	-8	3
-13	-1	-2	1
-10	2	1	1
-8	4	-1	5
12	23	22	1
-2	9	6	3
-7	4	4	0
2	12	11	1
-7	4	7	3
5	15	17	2
1	11	17	6
13	24	28	4
8	18	25	7
26	40	39	1
33	49	48	1
9	20	22	2
11	22	29	7
24	37	40	3
17	29	32	3
20	32	32	0
53	80	86	6
55	83	88	5
47	70	75	5
51	77	79	2
73	117	112	5

APPENDIX B

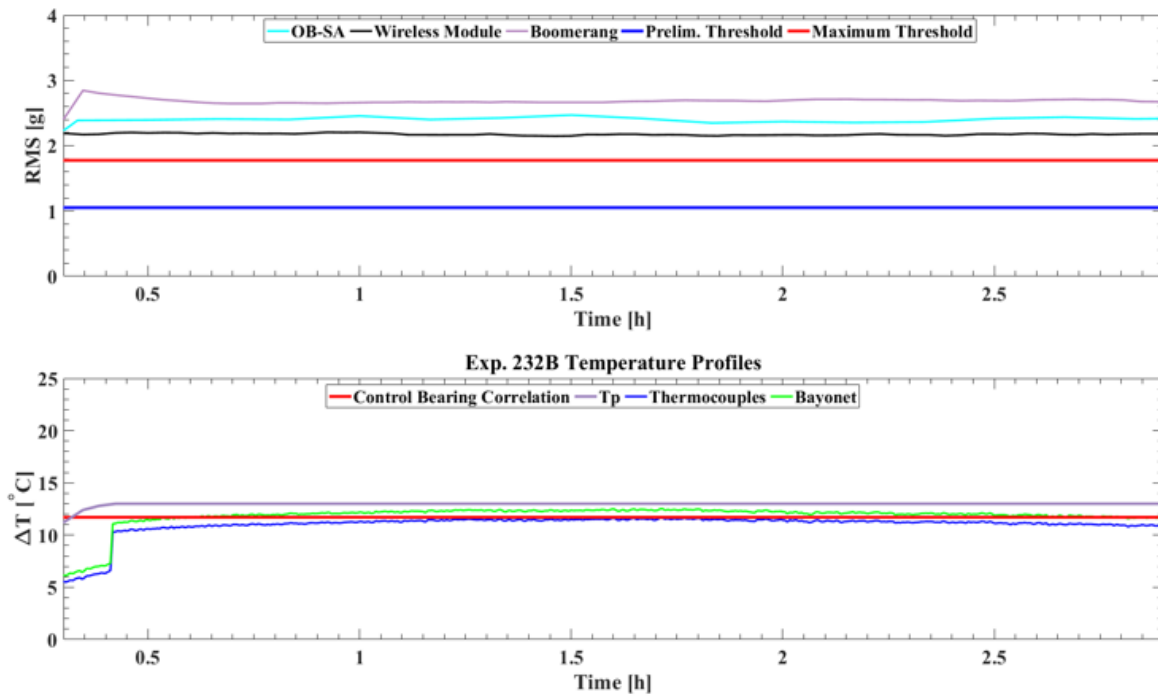SYSTEMATIC TESTING OF EXPERIMENT 232B

Figure B 1: Experiment 232 B, Boomerang C vibration and temperature profile for defective (cup spall) bearing operating at 40 km/h (25 mph) under 17% applied load (empty railcar)
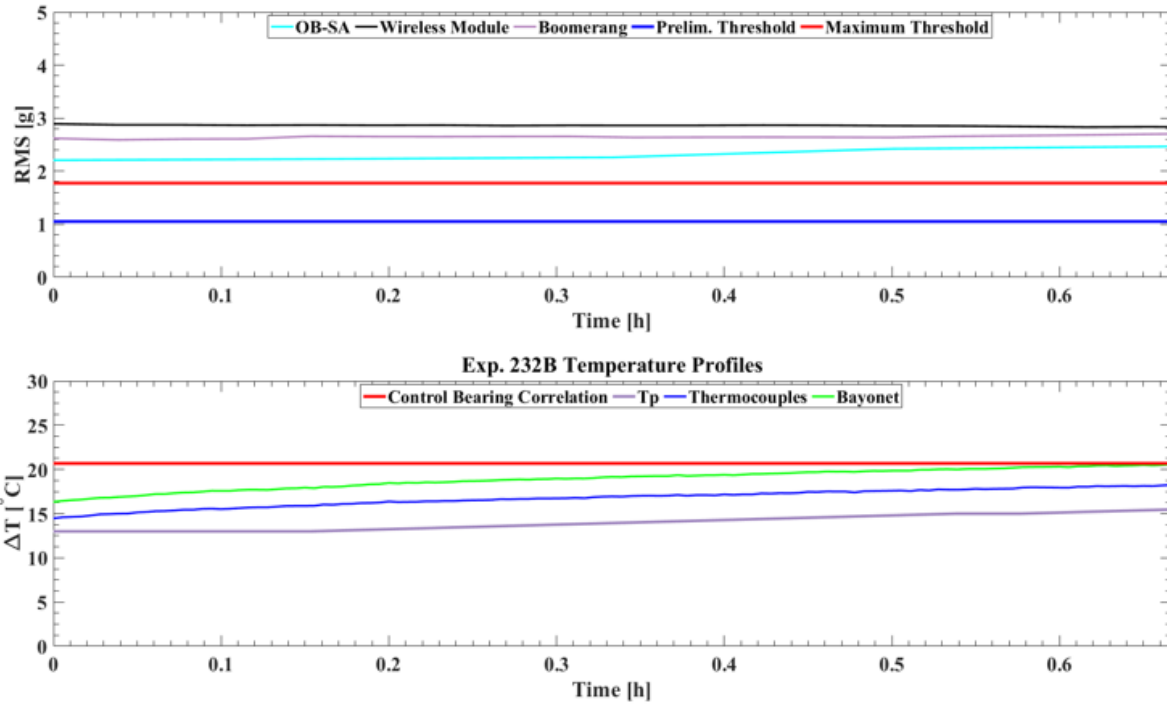
Figure B 2: Experiment 232 B, Boomerang C vibration and temperature profile for defective (cup spall) bearing operating at 40 km/h (25 mph) under 100% applied load (fully loaded railcar)
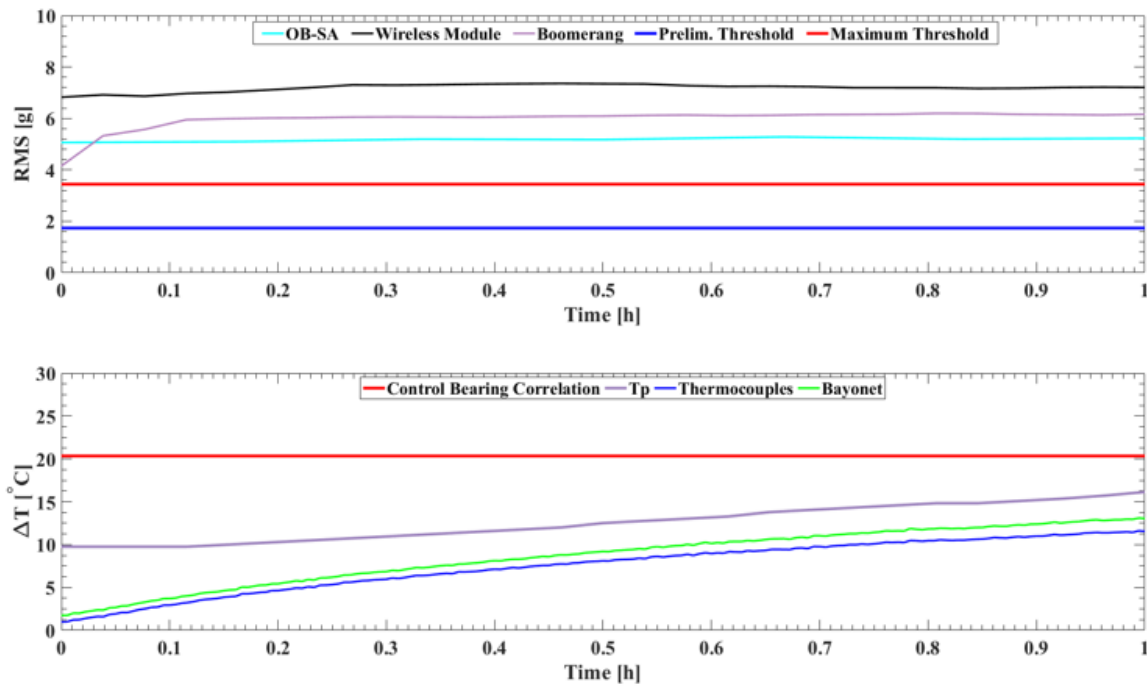

Figure B 3: Experiment 232 B, Boomerang C vibration and temperature profile for defective (cup spall) bearing operating at 64 km/h (40 mph) under 17% applied load (empty railcar)
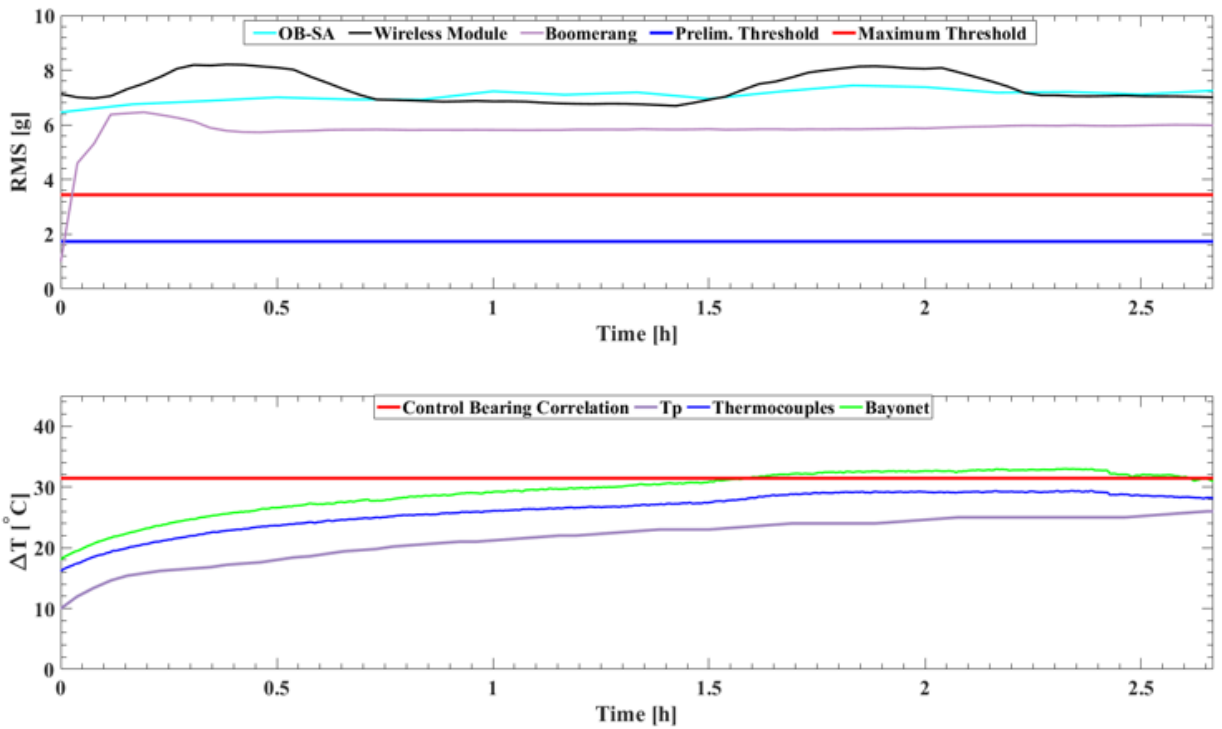
Figure B 4: Experiment 232 B, Boomerang C vibration and temperature profile for defective (cup spall) bearing operating at 64 km/h (40 mph) under 100% applied load (fully loaded railcar)
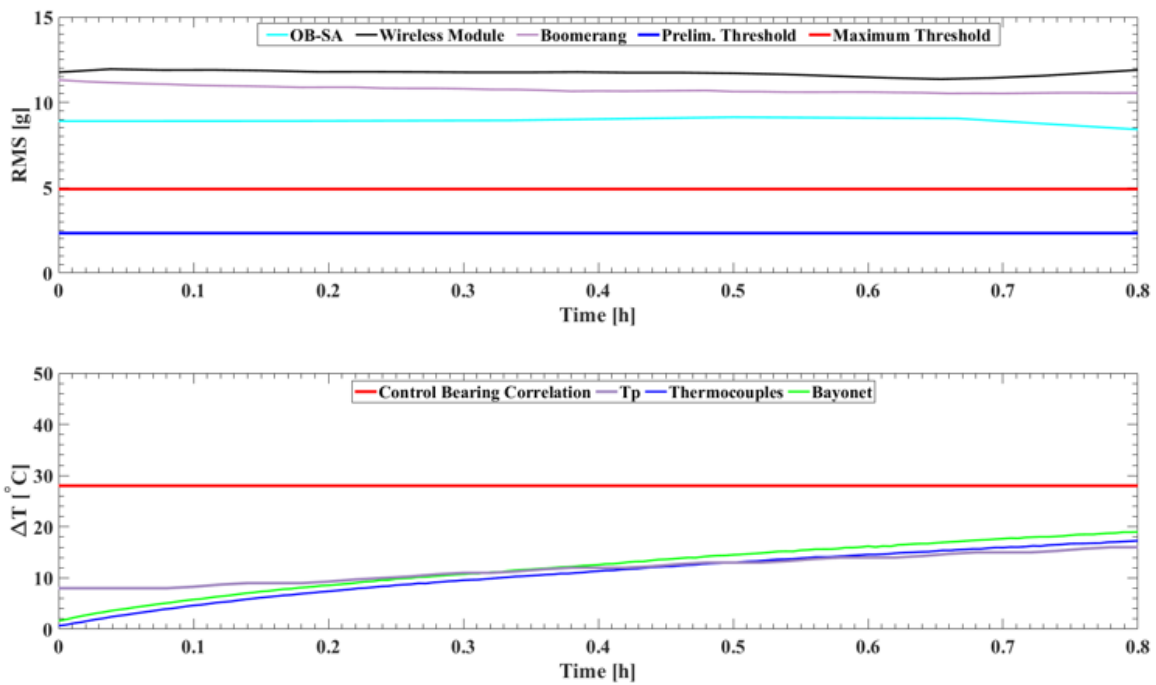

Figure B 5: Experiment 232 B, Boomerang C vibration and temperature profile for defective (cup spall) bearing operating at 85 km/h (53 mph) under 17% applied load (empty railcar)
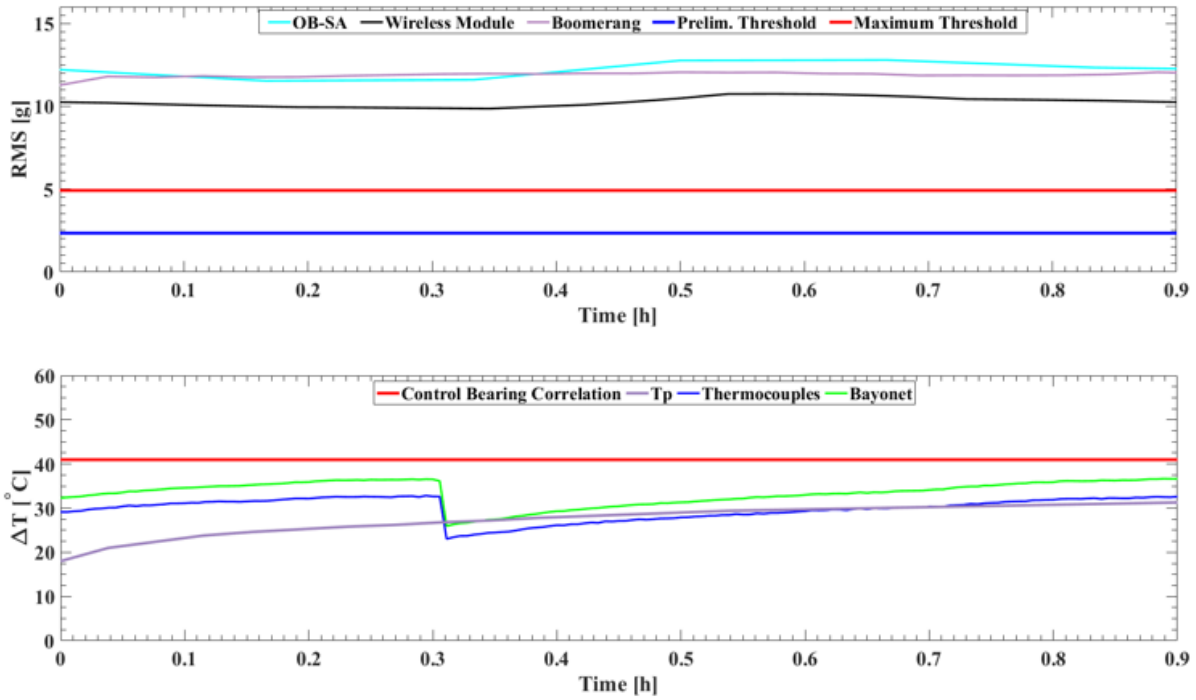
Figure B 6: Experiment 232 B, Boomerang C vibration and temperature profile for defective (cup spall) bearing operating at 85 km/h (53 mph) under 100% applied load (fully loaded railcar)

BIOGRAPHICAL SKETCH

Lee R. Cantu was born in McAllen, Texas, on October 3rd, 1996, to Flor and Edelmiro Cantu. He attended La Joya High School and graduated top 10 from his class in 2015. He pursued his educational career as an undergraduate student at the University of Texas Rio Grande Valley, where he graduated Summa Cum Laude with a bachelor's degree in Mechanical Engineering in December 2019. Lee received the mechanical engineering department outstanding student award in 2018 and numerous excellence scholarships throughout his educational career. Lee completed two internships as an undergraduate, one with NASA Johnson Space Center in the Power and Propulsion team in Spring 2019 and a 2019 summer internship with Cummins Inc. as a Quality Analytics Intern. In addition to his internships, Lee served as a laboratory assistant for engineering materials, heat transfer, and fluid dynamics. In addition to serving his university, he served as a Researcher Assistant to the Railroad Safety Research Team for three years. Lee continued his education and completed his Master of Science degree in Mechanical Engineering in December 2021. Lee can be reached by e-mail at lee.cantu01@gmail.com.